

CONFIDENTIAL

Copy  
RM E53E06

6

JUL 8 1953



# RESEARCH MEMORANDUM

ACCELERATION OF HIGH-PRESSURE-RATIO SINGLE-SPOOL  
TURBOJET ENGINE AS DETERMINED FROM COMPONENT  
PERFORMANCE CHARACTERISTICS

II - EFFECT OF COMPRESSOR INTERSTAGE AIR BLEED

By John J. Rebeske, Jr. and James F. Dugan, Jr.

Lewis Flight Propulsion Laboratory  
Cleveland, Ohio

CLASSIFIED DOCUMENT

This material contains information affecting the National Defense of the United States within the meaning of the espionage laws, Title 18, U.S.C., Sec. 793 and 794, the transmission or revelation of which in any manner to an unauthorized person is prohibited by law.

NATIONAL ADVISORY COMMITTEE  
FOR AERONAUTICS

WASHINGTON

July 3, 1953

CONFIDENTIAL

NACA LIBRARY  
NATIONAL ADVISORY COMMITTEE  
FOR AERONAUTICS  
WASHINGTON, D.C.  
UNCLASSIFIED

NACA RM E53E06

CLASSIFICATION CHANGED

To UNCLASSIFIED

By authority of *Naval PAB*  
*Effective Date 12-3-58*  
*NB 3-2-59*



3 1176 01435 7074

UNCLASSIFIED

F

NACA RM E53E06

~~CONFIDENTIAL~~

## NATIONAL ADVISORY COMMITTEE FOR AERONAUTICS

RESEARCH MEMORANDUM

## ACCELERATION OF HIGH-PRESSURE-RATIO SINGLE-SPOOL TURBOJET ENGINE

## AS DETERMINED FROM COMPONENT PERFORMANCE CHARACTERISTICS

## II - EFFECT OF COMPRESSOR INTERSTAGE AIR BLEED

By John J. Rebeske, Jr. and James F. Dugan, Jr.

## SUMMARY

An analytical investigation was made to determine the effect of compressor interstage air bleed with the use of constant-area bleed ports on the acceleration characteristics of a typical high-pressure-ratio single-spool turbojet engine. Constant-area interstage bleed, properly located, gave smaller acceleration times than variable-area compressor exit bleed. For constant effective bleed areas resulting in approximately equal amounts of bleed air flow, interstage bleed was most effective when it occurred at the middle or slightly to the rear of the middle of the compressor. Improved acceleration characteristics were obtained with a combination of compressor interstage and exit bleed. For this combination, acceleration along paths away from the surge line gave acceleration times only slightly larger than that for acceleration along the surge line.

## INTRODUCTION

Studies of turbojet-engine requirements for high-altitude transonic flight indicate the need for compressor pressure ratios of about 7 to 10 and turbine-inlet temperatures of 2000° to 2300° R (ref. 1). When a single-spool axial-flow compressor is used in this pressure-ratio range, it usually has poor off-design performance which results in poor engine acceleration characteristics. In the low-speed range from 50 to 80 per cent of design, the compressor inlet stages operate in a low-efficiency, high-angle-of-attack region and the outlet stages operate in a low-efficiency, low-angle-of-attack region (ref. 2).

Equilibrium operation of a typical high-pressure-ratio single-spool turbojet engine is described in reference 3. This reference shows that equilibrium engine operating lines of this particular compressor-turbine configuration enter the compressor surge-region in the intermediate speed range and that the engine will not accelerate through the compressor surge region. Therefore, the component performances of the compressor and turbine and/or the matching of these components must be altered to permit acceleration.

~~CONFIDENTIAL~~

UNCLASSIFIED

2916

1-10

Improved acceleration characteristics of such engines may result from the use of: compressor outlet bleed, which changes the matching of compressor and turbine; compressor interstage bleed, which changes the matching of compressor and turbine as well as the matching of stages within the compressor; adjustable compressor-inlet guide vanes and stators; and adjustable turbine stators. An investigation is being conducted at the NACA Lewis laboratory to evaluate the relative merit of each of the aforementioned schemes for improving the accelerating characteristics of high-pressure-ratio single-spool turbojet engines.

The first part of this investigation is reported in reference 4, in which the effect on acceleration time of turbine-inlet temperature and proximity to compressor surge with compressor outlet bleed is presented. The results of this investigation indicated that reasonable amounts of compressor outlet bleed permit high turbine-inlet temperatures during acceleration, and the acceleration path on the compressor map should be as close to the surge region as possible throughout the speed range. For the modes of acceleration considered, over 84 percent of the total acceleration time was required to accelerate through the low-speed range (50 to 80 percent of design). Consequently, improved low-speed compressor performance should give a significant reduction in acceleration time.

In comparison with compressor discharge bleed, which allows rematching of a given compressor and turbine, interstage compressor bleed has the additional advantage of allowing a rematching of the compressor stages themselves so that improved low-speed compressor performance may be obtained. The purpose of this report is to present the effect of constant-area interstage bleed on the calculated engine acceleration time.

Calculated compressor performance with interstage bleed is presented for bleed at the discharge of the 4<sup>th</sup>, 8<sup>th</sup>, and 12<sup>th</sup> stages. Correspondingly, acceleration times are presented for specified acceleration paths on the compressor maps. The acceleration time is also presented for a combination of interstage and exit bleed with a turbine-inlet temperature of 2500° R.

#### SYMBOLS

The following symbols are used in this report:

- A      area, sq in.
- A<sub>a</sub>    annulus area, sq ft
- c<sub>p</sub>    specific heat at constant pressure, Btu/(lb)(°R)

$c_v$	specific heat at constant volume, Btu/(lb)(°R)
$f$	ratio of fuel flow to air flow
$H'$	stagnation enthalpy, Btu/lb
$I$	polar moment of inertia, slug-ft <sup>2</sup>
$J$	mechanical equivalent of heat, 778.16 ft-lb/Btu
$K$	constant, $60 J/2\pi$ , (sec)(ft-lb)/(min)(Btu)
$M$	Mach number
$N$	rotative speed, rpm
$p$	static pressure, lb/sq ft
$p'$	stagnation pressure, lb/sq ft
$Q'$	volume flow based on stagnation density, cu ft/sec
$r$	radius, ft
$T'$	stagnation temperature, °R
$U$	blade velocity, ft/sec
$w$	weight flow, lb/sec
$\alpha$	angular acceleration, radians/sec <sup>2</sup>
$\Gamma$	torque, ft-lb
$\Gamma_a$	torque for accessories and friction losses, ft-lb
$\gamma$	ratio of specific heats, $c_p/c_v$
$\delta$	ratio of stagnation pressure to pressure at NACA standard sea-level conditions, $p'/2116$
$\eta$	adiabatic efficiency, percent
$\theta$	ratio of stagnation temperature to temperature at NACA standard sea-level conditions, $T'/518.4$

$\rho$  density, lb/cu ft  
 $\tau$  time, sec  
 $\omega$  angular velocity, radians/sec

Subscripts:

0 NACA standard sea-level conditions  
1 compressor inlet  
2 compressor outlet  
3 turbine inlet  
4 turbine outlet  
5 exhaust nozzle  
II inlet of stages 5 to 8  
III inlet of stages 9 to 12  
IV inlet of stages 13 to 16  
b bleed  
c compressor  
d design  
e equivalent  
i idle  
l leakage  
m mean  
n inlet of rotor  
o outlet of rotor  
s isentropic  
t turbine

## METHODS AND PROCEDURES

In the calculation of the acceleration times, it was assumed that NACA standard sea-level conditions existed at the compressor inlet, that actual compressor performance with interstage bleed would be the same as that calculated from stage group performance curves, and that steady-state compressor and turbine performance is obtained during acceleration; in addition, the following assumptions were made:

Ram pressure ratio, $p_1/p_0$ . . . . .	1.0
Burner pressure ratio, $p_3'/p_2'$ . . . . .	0.97
Stagnation pressure loss in tail pipe for $M_5 = 1.0$ , $p_5'/p_4'$ . .	0.97
Fuel equal to air leakage between the compressor and the turbine, $fw_{c,2}$ . . . . .	$w_l$
Gamma for gas flow in turbine and tail pipe, $\gamma$ . . . . .	1.32
Maximum allowable turbine-inlet temperature, $T_3'$ . . . . .	2500° R
Torque for accessories and friction losses, $\Gamma_a/\delta_3$ , ft-lb . . . .	3.0
Exhaust-nozzle area, $A_5$ , sq in. . . . .	600

Compressor performance. - The performance of the 16-stage axial-flow compressor used in this investigation is presented in reference 2, in which the compressor is designated configuration A. Its over-all performance appears in figure 1 as a plot of total-pressure ratio and adiabatic efficiency against corrected weight flow for constant values of corrected speed. The stage group performance data are presented in figure 2, in which equivalent temperature-rise ratio and equivalent pressure ratio are plotted against flow coefficient. Curves of constant compressor corrected speed were faired through these data points and extrapolated. The over-all compressor performance without interstage bleed was calculated using these faired curves and the "stacking" method presented in appendix A, which is essentially the same as that reported in reference 5. This calculated performance is presented in figure 3 so that it can be compared with the experimental performance. The two performance maps differ only slightly, which is an indication of the validity of the faired lines of constant speed through the stage group performance data. Over-all compressor performance for operation with interstage bleed was also calculated by using the stage group performance data (fig. 2) and the stacking method. The validity of the performance maps obtained in this manner was not experimentally verified.

In general, the procedure used to calculate the compressor performance with interstage bleed was to reduce the flow coefficient ( $Q'/U_m A_a$ ) entering a given stage group in proportion to the amount of air bleed desired and to assume that the stage group performance would be that obtained from the stage group data of figure 2 using the reduced flow coefficient. The amount of air bleed was selected as approximately

10 percent of the compressor-inlet weight flow in the intermediate speed range (70 to 80 percent corrected design speed). The effective areas required to bleed this amount of air were calculated for bleed at the discharge of the 12th, 8th, and 4th compressor stages. With the effective bleed area known, the corresponding compressor performance was calculated over a range of speeds from 50 to 100 percent of design. Further discussion of the method is presented in appendix A. The compressor performance thus calculated is presented in figure 4, in which compressor pressure ratio and efficiency are plotted against corrected weight flow ( $w_{c,2} \sqrt{\theta_1/\delta_1}$ ) for lines of constant corrected speed.

Modes of engine operation. - In order to evaluate the effect of compressor interstage bleed on acceleration time, engine acceleration paths were arbitrarily specified at constant percentage values of surge pressure ratio (except when  $T_3^* >$  the maximum allowable value of  $2500^\circ \text{R}$ ).

These lines of constant percentage values of surge pressure ratio are presented in figure 5, in which compressor pressure ratio is plotted against a weight-flow parameter for lines of constant corrected speed. The mode of engine operation along these specified acceleration paths was considered to be as follows: Zero time was taken as equilibrium engine operation at idle speed, approximately 50 percent of design, with the exhaust nozzle wide open. Instantaneously the engine operated at the idle speed terminus of one of the specified acceleration paths. As the engine accelerated along the specified path, the turbine-inlet temperature varied continuously. When an engine speed was reached that no longer required interstage compressor bleed to stay out of the compressor surge with  $T_3^*$  equal to  $2500^\circ \text{R}$ , the air bleed was stopped instantaneously and the engine acceleration then proceeded along the line of  $T_3^* = 2500^\circ \text{R}$  until 100 percent corrected design speed was attained.

The exhaust-nozzle area was then decreased until equilibrium operation at design  $T_3^*$  ( $2160^\circ \text{R}$ ) was achieved.

For the case in which compressor discharge bleed is combined with interstage bleed, a similar mode of engine operation is specified. The only difference is that  $T_3^*$  is held constant at  $2500^\circ \text{R}$  and the amount of compressor outlet bleed is varied to attain compressor operation along the specified acceleration paths.

Determination of acceleration times. - The method employed to determine the acceleration times is described in reference 4. For convenience, it is restated here. The excess torque and acceleration are related by

$$\Delta \Gamma = \Gamma_t - (\Gamma_c + \Gamma_a) = I \alpha = I \frac{d\omega}{dt} \quad (1)$$

Solving for the time required to achieve a given change in angular velocity yields

$$\int_{\tau_i}^{\tau_d} d\tau = I \int_{\omega_i}^{\omega_d} \frac{d\omega}{\Gamma_t - (\Gamma_c + \Gamma_a)} = \frac{2\pi}{60} \frac{I N_d}{100} \int_{\left(100 \frac{N_i}{N_d}\right)}^{100} \frac{d\left(100 \frac{N}{N_d}\right)}{\Delta \Gamma} \quad (2)$$

If the excess torque  $\Delta \Gamma$  developed by the turbine over that required by the compressor, accessories, and friction losses can be expressed as a function of engine rpm, equation (2) may be integrated and the corresponding time required for a given change in engine rpm evaluated. The excess torque is obtained from compressor and turbine maps such as those presented in figures 6 and 7.

The particular procedure used to calculate the excess torque is outlined in appendix B.

## RESULTS AND DISCUSSION

The results obtained from the present investigation are dependent upon the validity of the calculated compressor performance with interstage bleed. However, the results are believed to be indicative of the relative merit of using constant-area interstage bleed for avoiding surge and shortening the required engine acceleration times.

The amount of interstage air bleed was selected as approximately 10 percent of compressor-inlet weight flow in the intermediate speed range (70 to 80 percent corrected design speed). The effective areas required to bleed this amount of air were calculated to be 9.5, 12.0, and 17.5 square inches for bleed at the discharge of the 12th, 8th, and 4th compressor stages, respectively. Use of constant-area interstage bleed results in a variation of bleed air with compressor speed. The variation of the ratio of bleed air flow to compressor design air flow with compressor speed for operation along the surge line and bleed at the exit of the 12th, 8th, and 4th stages is shown in figure 8. In the speed range from 50 to 80 percent corrected design speed, the maximum variation in this bleed ratio is less than 1 percent for the three bleed locations. Therefore, the relative merit of the three interstage bleed locations is evaluated for constant effective bleed areas resulting in approximately equal amounts of bleed air flow.

Acceleration with interstage bleed. - Acceleration times were calculated for interstage bleed at the outlet of the 12th, 8th, and 4th compressor stages along the specified acceleration paths shown in



figures 5(a), (b), and (c), respectively. These acceleration times are shown in figure 9, in which the acceleration time is plotted in seconds against percent of corrected design speed for lines of constant percentage values of surge pressure ratio. The time required to accelerate to any given speed increases as the specified acceleration paths move to lower percentage values of surge pressure ratio and as the interstage bleed point moves from the 12th to the 4th compressor stage. Again, as indicated in reference 4, a large percentage of the total acceleration time is required to accelerate from 50 to 80 percent of corrected design speed for all specified acceleration paths. The time required to accelerate from 80 to 100 percent of corrected design speed remains essentially constant as indicated by the slopes of the specified operating lines in this speed range.

A comparison of the total acceleration times for bleed at the outlet of the 12th, 8th, and 4th compressor stages is presented in figure 10, in which total acceleration time is plotted against percent of surge pressure ratio. There is relatively little difference in the total acceleration times for bleed at the 12th and 8th stages, particularly at higher percentage values of surge pressure ratio. Total acceleration times for bleed at the 4th stage are significantly higher and increase rapidly as the percent of surge pressure ratio decreases.

Engine acceleration along the specified acceleration paths with compressor interstage bleed alone required a specific variation in turbine-inlet temperature with engine speed. This variation of turbine-inlet temperature for acceleration along the compressor surge lines is presented in figure 11 for bleed at the 12th, 8th, and 4th compressor stages. Examination of the figure indicates that the turbine-inlet temperatures required fall below the maximum allowable ( $2500^{\circ}$  R). Turbine-inlet temperatures for engine acceleration paths at lower percentage values of surge pressure ratio would be even lower than the values shown for the surge case.

The acceleration characteristics will be improved if the deviations from the maximum allowable turbine-inlet temperature ( $2500^{\circ}$  R) can be reduced. This might be accomplished by various means. If compressor exit bleed is employed in combination with constant-area interstage bleed, it is possible to specify a turbine-inlet temperature of  $2500^{\circ}$  R for all acceleration paths considered. If more air can be bled from interstage bleed points than was previously considered without adversely affecting compressor performance, the deviation from the maximum allowable turbine-inlet temperature ( $2500^{\circ}$  R) will be reduced for a specified path. If variable-area interstage bleed is used, a turbine-inlet temperature of  $2500^{\circ}$  R may be specified for all acceleration paths considered.

2916

Acceleration using constant-area interstage bleed in combination with compressor outlet bleed. - The effect on engine acceleration of combining variable-area compressor outlet bleed with constant-area interstage bleed is presented in figure 12. Total acceleration times are plotted against percent of surge pressure ratio for a combination of variable-area compressor outlet bleed and interstage bleed at the 12<sup>th</sup>, 8<sup>th</sup>, and 4<sup>th</sup> compressor stages. Total acceleration times for bleed at the 12<sup>th</sup> and 8<sup>th</sup> stages are essentially the same, and the acceleration times for bleed at the 4<sup>th</sup> stage are only slightly greater. However, the important fact to note is that the slope of the bleed lines is small. This means that such an engine could be scheduled to accelerate at lower percentage values of surge pressure ratio without paying a large penalty in total acceleration time, thus decreasing the danger of surging the compressor during acceleration. The use of exit bleed to maintain  $T_{\frac{1}{2}}$  equal to 2500° R would require a control to provide a continuously varying bleed area at the compressor discharge.

CT-2

In an effort to simplify the exit-area control, engine acceleration times were calculated with simple step-area variations for the bleed at the compressor outlet. The required area variations for compressor outlet bleed are shown in figures 13(a), (b), and (c) for interstage bleed at the 12<sup>th</sup>, 8<sup>th</sup>, and 4<sup>th</sup> compressor stages, respectively. In figure 13(a) the area variation is plotted against percent of corrected compressor design speed for constant percentage values of surge pressure ratio. Also shown are the specified step-area variations for which the acceleration times were calculated. A single step-area (constant area) compressor outlet bleed was not considered because it would move the resulting engine acceleration path too far away from the original acceleration path with a corresponding increase in total acceleration time. For example, by specifying a two-step-area variation for the surge case, the engine acceleration path stays relatively near the compressor surge line, never falling below 99 percent of surge pressure ratio for engine speeds below 77.5 percent of corrected design speed. At speeds above 77.5 percent corrected design speed, the specified acceleration paths do fall to lower percentages of surge pressure ratio; this is not serious since only a small percent of the total acceleration time is spent in this speed range. Step-area variations were similarly specified for all other engine accelerations considered.

The effect on engine acceleration of combining step-area compressor outlet bleed with constant-area interstage bleed is presented in figure 14. Total acceleration times are plotted against percent of surge pressure ratio for interstage bleed at the 4<sup>th</sup>, 8<sup>th</sup>, and 12<sup>th</sup> compressor stages in combination with step-area bleed at the compressor discharge. Total acceleration times for bleed at the 12<sup>th</sup> and 8<sup>th</sup> stages are essentially the same, and the acceleration times for the 4<sup>th</sup> stage are 1 to 2 seconds longer.

Effect of amount of air bleed on acceleration using constant-area interstage bleed at exit of 12<sup>th</sup> compressor stage. - As stated previously, the amount of air bleed was selected as approximately 10 percent of the compressor-inlet weight flow in the intermediate speed range (70 to 80 percent corrected design speed). If more air can be bled without adversely affecting compressor performance, improved acceleration characteristics will result.

The effect of the amount of bleed on total acceleration time is shown in figure 15. Total acceleration time is plotted against effective bleed area at the outlet of the 12<sup>th</sup> compressor stage for acceleration paths specified by constant percentage values of surge pressure ratio. Because the engine will not accelerate through the compressor surge region, the total acceleration time for no interstage bleed (zero area) is infinite. Examination of the figure reveals that as effective bleed area increases the total acceleration time decreases and the change in acceleration time for the specified acceleration paths decreases. In practice, the amount of interstage bleed will probably be limited to a value beyond which the performance of stages near the bleed location will be seriously affected. Such a limiting bleed area can best be evaluated experimentally. The largest bleed area considered is 13 square inches. Calculation of compressor performance for larger bleed areas would require doubtful extrapolations of the curves through the compressor stage group data (fig. 2). Moreover, because the slopes of the curves in figure 15 are very small at 13 square inches, only slight improvements in acceleration characteristics can be expected for bleed ports larger than 13 square inches.

Variable-area interstage bleed. - There is a strong possibility that a continuously variable area or a step-area interstage bleed that would maintain a turbine-inlet temperature of 2500° R during acceleration would give smaller acceleration times than those calculated for constant-area interstage bleed. Because of the probable significant effects on compressor performance of the large values of bleed air flow required, this mode of interstage bleed was not considered in the present analytical investigation.

Comparison of acceleration modes. - The different modes of engine acceleration considered in this investigation and in reference 4 are summarized in figure 16. Total acceleration time is plotted against the mode of engine acceleration for acceleration paths specified by constant percentages of surge pressure ratio. The merit of a particular acceleration mode may be judged by the magnitude of the total acceleration time, by the increase in total acceleration time required by specifying acceleration at lower percentages of surge pressure ratio, and by the complexity of the necessary engine controls.

By comparing modes 6, 7, and 12 with modes 2 and 3, it is evident that constant-area interstage bleed properly located gives smaller acceleration times than compressor outlet bleed. Comparison of modes 1, 6, and 7 reveals that, for constant effective bleed areas resulting in approximately equal amounts of bleed air flow, compressor interstage air bleed at the 8th and 12th compressor stages gave significantly smaller acceleration times than air bleed at the 4th compressor stage. By comparing modes 1, 6, and 7 with modes 4, 5, 8, 9, 10, and 11, it is evident that improved acceleration characteristics were obtained by combining compressor outlet bleed with constant-area interstage bleed such that the turbine-inlet temperature is 2500° R. By comparing modes 8 and 9 with modes 10 and 11, it is seen that specifying a step-area variation in place of a continuously varying area at the compressor outlet in combination with a constant-area interstage bleed at the 8th or 12th compressor stage required no significant increases in acceleration times. Modes 8, 9, 10, and 11 also show that the combination of interstage bleed at the 8th or 12th compressor stage with compressor discharge bleed required only small increases in acceleration time for acceleration at lower percentages of surge pressure ratio.

#### SUMMARY OF RESULTS

From an analytical investigation to determine the effect of constant-area compressor interstage air bleed on the acceleration characteristics of a typical high-pressure-ratio single-spool turbojet engine, the following results were obtained:

1. Constant-area interstage bleed, properly located, gave smaller acceleration times than variable-area compressor exit bleed.
2. For constant effective bleed areas resulting in approximately equal amounts of bleed air flow, compressor interstage air bleed at the 8th and 12th compressor stages gave significantly smaller acceleration times than air bleed at the 4th compressor stage.
3. Improved acceleration characteristics were obtained by a combination of interstage bleed with a variable bleed area at the compressor outlet such that the turbine-inlet temperature was 2500° R.
4. Specifying a step-bleed-area variation in place of a continuously varying area at the compressor outlet in combination with a constant-area interstage bleed at the 8th or 12th compressor stage required no significant increase in acceleration times.

5. The combination of interstage bleed at the 8<sup>th</sup> or 12<sup>th</sup> compressor stages with compressor discharge bleed required only small increases in acceleration time for acceleration at lower percentages of surge pressure ratio.

Lewis Flight Propulsion Laboratory  
National Advisory Committee for Aeronautics  
Cleveland, Ohio, April 15, 1953

2916

## APPENDIX A

## METHOD FOR OBTAINING COMPRESSOR PERFORMANCE FROM STAGE

## GROUP PERFORMANCE DATA

In reference 2 (appendix A) the equivalent pressure ratio, equivalent temperature-rise ratio, and flow coefficient  $\varphi_m$  are derived for a compressor stage and can be expressed as

$$\varphi_m = \left( \frac{Q'}{U_m A_a} \right)_n \quad (A1)$$

$$\left( \frac{\Delta T}{T_n} \right)_e = f_1(\varphi_m) \quad (A2)$$

$$\left( \frac{P_o'}{P_n'} \right)_e = f_2(\varphi_m) \quad (A3)$$

The equivalent temperature-rise ratio and equivalent pressure ratio are those that would exist in a compressor stage for any given flow coefficient at design speed within the limits of the assumptions listed in appendix A of reference 2.

In reference 2, the equivalent performance parameters were computed for four groups of four stages each. Because the method of obtaining these parameters is based on a one-dimensional vector diagram for a single blade row, the stage group curves cannot be independent of speed. The stage group performance data are presented in figure 2 (fig. 5 of ref. 2). The flow coefficient is that at the inlet to the group of stages under consideration, and the equivalent speed ratio used to obtain the equivalent performance parameters is also that at the inlet to the groups of stages.

Calculated compressor performance without interstage bleed. - Lines of constant corrected speed were faired through the data points of figure 2. A value of  $\varphi_m$  for the first group of four stages may be calculated by selecting a weight flow  $w\sqrt{\theta_1}/\delta_1$  and corrected speed  $N/\sqrt{\theta_1}$

$$\varphi_{m,1} = \left( \frac{w\sqrt{\theta_1}}{\delta_1} \right) \frac{(N/\sqrt{\theta_1})_d}{(N/\sqrt{\theta})} k_1 \quad (A4)$$

where

$$k_1 = \frac{1}{\rho_0 A_{a,1} (r_{m,1}) \frac{2\pi}{60} (N/\sqrt{\theta_1})_d}$$

With the value of  $\varphi_{m,1}$  and the compressor corrected speed known, the equivalent temperature-rise ratio  $(\Delta T'/T'_1)_e$  and pressure ratio  $(p'_{11}/p'_1)_e$  are read from the appropriate faired speed line through the compressor data (fig. 2(a)). The actual values of  $\Delta T'/T'_1$  and  $p'_{11}/p'_1$  are computed by correcting the equivalent values for  $N/\sqrt{\theta_1}$

$$\frac{\Delta T'}{T'_1} = \left( \frac{\Delta T'}{T'_1} \right)_e \frac{(N/\sqrt{\theta_1})^2}{(N/\sqrt{\theta_1})_d^2} \quad (A5)$$

$$\frac{p'_{11}}{p'_1} = \left\{ \frac{(N/\sqrt{\theta_1})^2}{(N/\sqrt{\theta_1})_d^2} \left[ \left( \frac{p'_{11}}{p'_1} \right)_e^{\frac{\gamma-1}{\gamma}} - 1 \right] + 1 \right\}^{\frac{\gamma}{\gamma-1}} \quad (A6)$$

The value of  $\varphi_{m,II}$  entering the second group of four stages is determined from

$$\varphi_{m,II} = \varphi_{m,1} \left( \frac{k_{II}}{k_1} \right) \left( \frac{p'_1}{p'_{11}} \right) \left( \frac{T'_{11}}{T'_1} \right) \quad (A7)$$

where

$$k_{II} = \frac{1}{\rho_0 (A_{a,II}) r_{m,II} \frac{2\pi}{60} (N/\sqrt{\theta_1})_d}$$

The equivalent values of  $\Delta T'/T'_{II}$  and  $p'_{III}/p'_{II}$  are now read from the appropriate faired curves (fig. 2(b)). The actual values of  $\Delta T'/T'_{II}$  and  $p'_{III}/p'_{II}$  are then calculated

$$N/\sqrt{\theta_{II}} = (N/\sqrt{\theta_1}) \sqrt{T_1/T_{II}} \quad (A8)$$

$$\frac{\Delta T'}{T'_{II}} = \left( \frac{\Delta T'}{T'_{II}} \right)_e \frac{(N/\sqrt{\theta_{II}})^2}{(N/\sqrt{\theta_{II}})_d^2} \quad (A9)$$

$$\frac{P_{III}^i}{P_{II}^i} = \left\{ \frac{(N/\sqrt{\theta_{II}})^2}{(N/\sqrt{\theta_{II}})_d^2} \left[ \left( \frac{P_{III}^i}{P_{II}^i} \right)_e^{\frac{\gamma-1}{\gamma}} - 1 \right] + 1 \right\}^{\frac{\gamma}{\gamma-1}} \quad (A10)$$

The actual pressure and temperature ratios across the remaining groups of stages are calculated in a similar manner, and the over-all compressor pressure and temperature ratios are the products of all the individual stage group values.

The performance calculated from the test data of figure 2 and the experimentally determined performance (fig. 1) are presented in figure 3. The calculated surge line is determined by the peak pressure ratio of each speed curve. Portions of the speed curves to the left of the peak pressure ratios were calculated by extrapolating the faired speed curves of figure 2. The agreement between the calculated and the experimental performance is quite good.

Calculated compressor performance with interstage bleed. - Compressor performance with interstage bleed was calculated by the method discussed in the previous section. The flow coefficient at the entrance of the stage group was reduced by an amount corresponding to the amount of air bled. It was assumed that the stage group performance would be that obtained from the stage group data of figure 2 using the reduced flow coefficient.

Compressor adiabatic efficiency for operation with interstage bleed. - The compressor adiabatic efficiency for operation with interstage bleed is defined by the following equation:

$$\eta = \frac{w_{c,2}(H_2^i - H_1^i)_s}{w_{c,1}(H_b^i - H_1^i) + w_{c,2}(H_2^i - H_b^i)} \quad (A11)$$



## APPENDIX B

## PROCEDURE FOR CALCULATING EXCESS TORQUE

The particular procedure used to calculate the excess torque may be outlined as follows:

1. A point on a constant compressor speed line is chosen arbitrarily at some percent of compressor pressure ratio at surge (fig. 5). Corresponding values of  $p_2'/p_1'$  and  $w_{c,2}N/60\delta_2$  are read. For the given assumptions of fuel-air ratio  $f$ , engine leakage  $w_l$ , and burner pressure drop  $\delta_3/\delta_2$ , a value of  $w_tN/60\delta_3$  may be calculated from the following equation:

$$\frac{w_tN}{60\delta_3} = \left( 1 + f - \frac{w_l}{w_{c,2}} \right) \frac{\delta_2}{\delta_3} \frac{w_{c,2}N}{60\delta_2} \quad (B1)$$

This value of  $w_tN/60\delta_3$  is the weight-flow parameter the turbine would have for the compressor to operate at the particular point chosen.

2. The corresponding value of torque  $(\Gamma_c/\delta_3 + \Gamma_a/\delta_3)$  required by the compressor, accessories, and friction losses is shown in figure 6 as a function of the normal turbine weight-flow parameter  $w_tN/60\delta_3$  for lines of constant compressor speed. The torque required for the particular point is determined by the compressor speed and the weight-flow parameter  $w_tN/60\delta_3$ .

3. The variation of turbine torque is shown in figure 7 as a function of  $w_tN/60\delta_3$  for lines of constant turbine speed and pressure ratio. With the compressor speed and weight-flow parameter known for the particular point chosen, several values of  $\Gamma_t/\delta_3$ ,  $p_3/p_4$ , and  $\frac{N/\sqrt{\theta_3}}{(N/\sqrt{\theta_3})_d}$  are read along a line of constant  $w_tN/60\delta_3$ .

4. A trial-and-error solution for the turbine torque is now required. With the use of the values of turbine torque, pressure ratio, corrected speed, and compressor pressure ratio, values of  $p_4/p_0$ ,  $p_4$ ,  $T_3$ ,  $T_4$ , and  $w_t$  are calculated from the following equations:

$$\frac{T_3'}{T_1'} = \left( \frac{N/\sqrt{\theta_1}}{N/\sqrt{\theta_3}} \right)^2 \quad (B2)$$

$$\frac{p_4'}{p_0} = \frac{p_2'}{p_0} \frac{p_3'}{p_2'} \frac{p_4'}{p_3'} \quad (B3)$$

$$\frac{T_4'}{T_3'} = 1 - \frac{\Gamma_t N}{K w_t c_p T_3'} \quad (B4)$$

$$w_t = \frac{w_t N}{60 \delta_3} \left( \frac{60 \delta_3}{N} \right) \quad (B5)$$

The exhaust-nozzle area is then calculated as described in reference 4 and plotted against  $p_3'/p_4'$ . The value of  $p_3'/p_4'$  corresponding to the assumed value of  $A_5$  (600 sq in.) is thus determined. From this value of  $p_3'/p_4'$  and  $w_t N/60 \delta_3$ ,  $\Delta \Gamma$  is determined. This procedure holds for cases where  $T_3' \leq 2500^\circ \text{R}$ ; if, however,  $T_3' > 2500^\circ \text{R}$ , it is necessary to modify the procedure in the following manner: The turbine-inlet stagnation temperature  $T_3'$  is assumed equal to  $2500^\circ \text{R}$  and, together with the known compressor speed,  $N/\sqrt{\theta_3}$  is determined. Several values of turbine torque, pressure ratio, and  $w_t N/60 \delta_3$  are read from the line of constant  $N/\sqrt{\theta_3}$ . For each of these values, the corresponding compressor torque and pressure ratio are determined and the solution follows the steps that have been previously outlined.

5. A graphical integration of equation (2) is obtained by plotting  $1/\Delta \Gamma$  against  $100N/N_d$  for the specified engine operating line.

6. For the case of exit bleed together with interstage bleed, the procedure is the same as outlined in reference 4.

## REFERENCES

1. Lubarsky, Bernard: Performance and Load-Range Characteristics of Turbojet Engine in Transonic Speed Range. NACA TN 2088, 1950.
2. Medeiros, Arthur A., Benser, William A., and Hatch, James E.: Analysis of Off-Design Performance of a 16-Stage Axial-Flow Compressor with Various Blade Modifications. NACA RM E52I03, 1953.
3. Rebeske, John J., Jr., and Dugan, James F., Jr.: Matched Performance Characteristics of a 16-Stage Axial-Flow Compressor and a 3-Stage Turbine. NACA RM E52H18, 1953.
4. Rebeske, John J., Jr., and Rohlik, Harold E.: Acceleration of High-Pressure-Ratio Single-Spool Turbojet Engine as Determined from Component Performance Characteristics. I - Effect of Air Bleed at Compressor Outlet. NACA RM E53A09, 1953.
5. Finger, Harold B., and Dugan, James F., Jr.: Analysis of Stage Matching and Off-Design Performance of Multistage Axial-Flow Compressors. NACA RM E52D07, 1952.

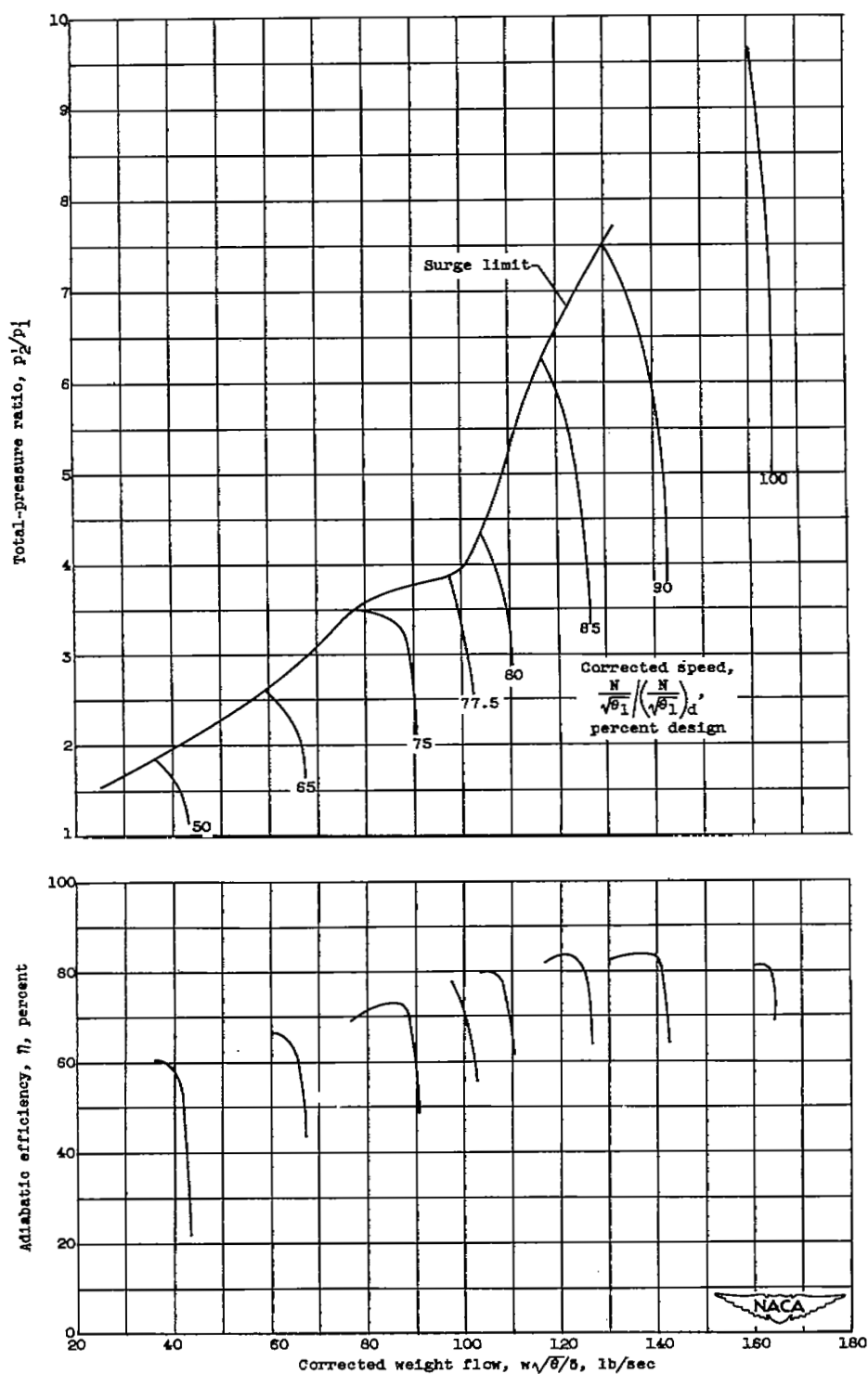
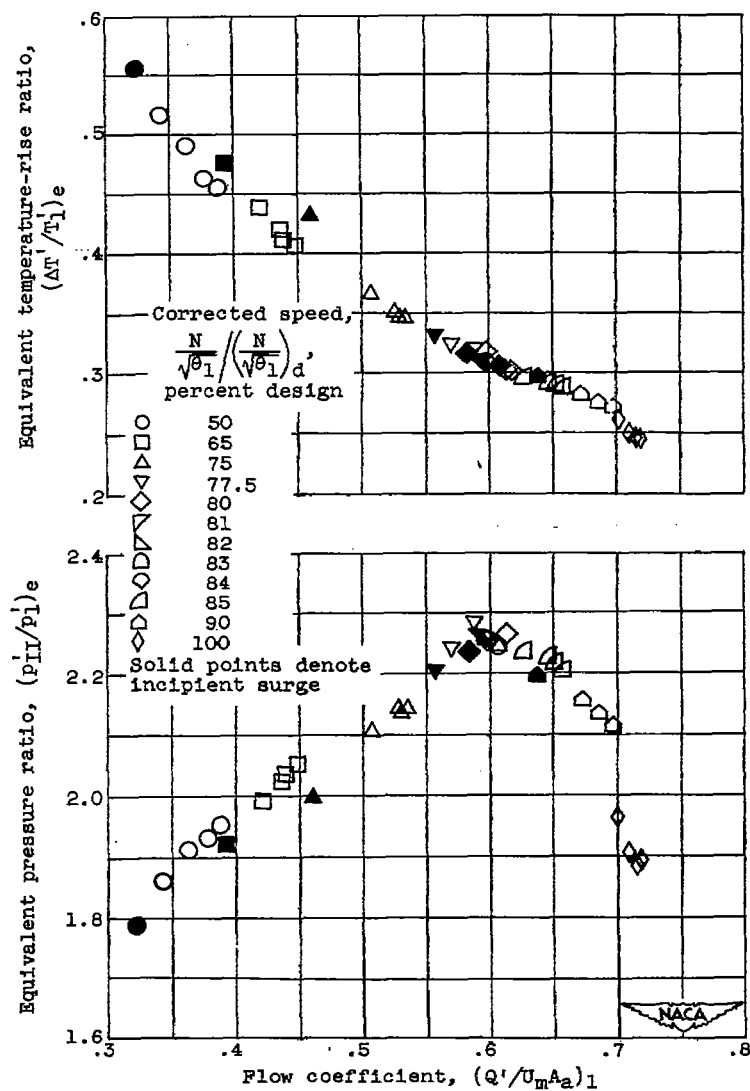
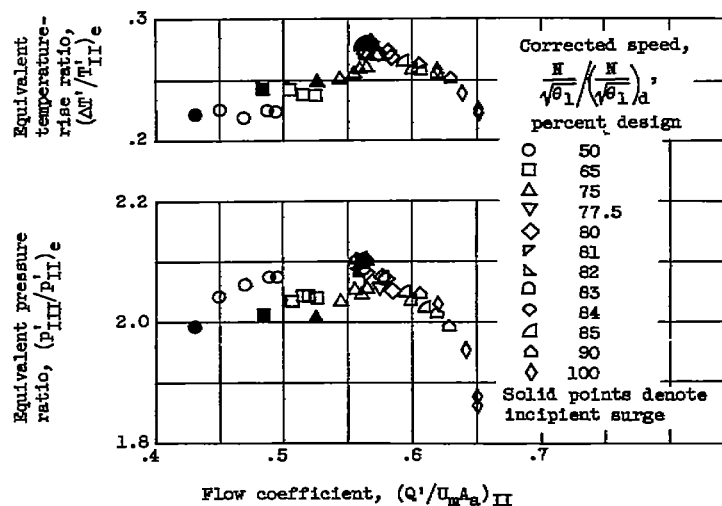


Figure 1. - Over-all performance of a 16-stage axial-flow compressor.



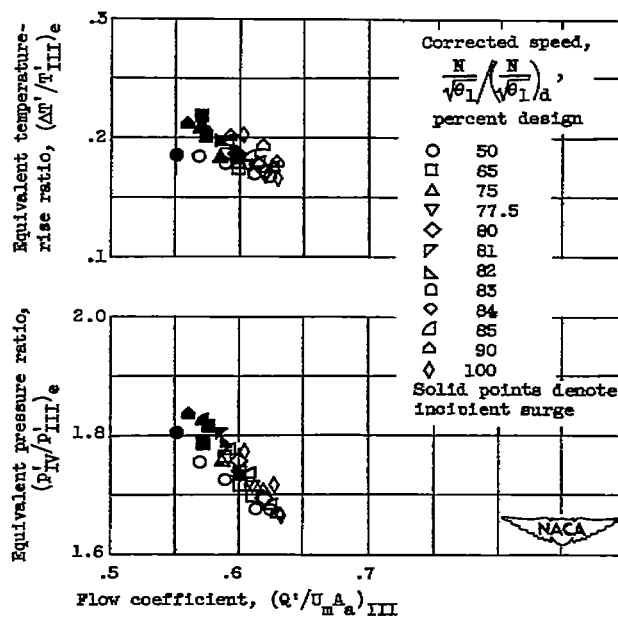
(a) Stages 1 to 4.

Figure 2. - Stage group performance for a 16-stage axial-flow compressor.



(b) Stages 5 to 8.

Figure 2. - Continued. Stage group performance for a 16-stage axial-flow compressor.



(c) Stages 9 to 12.

Figure 2. - Continued. Stage group performance for a 16-stage axial-flow compressor.

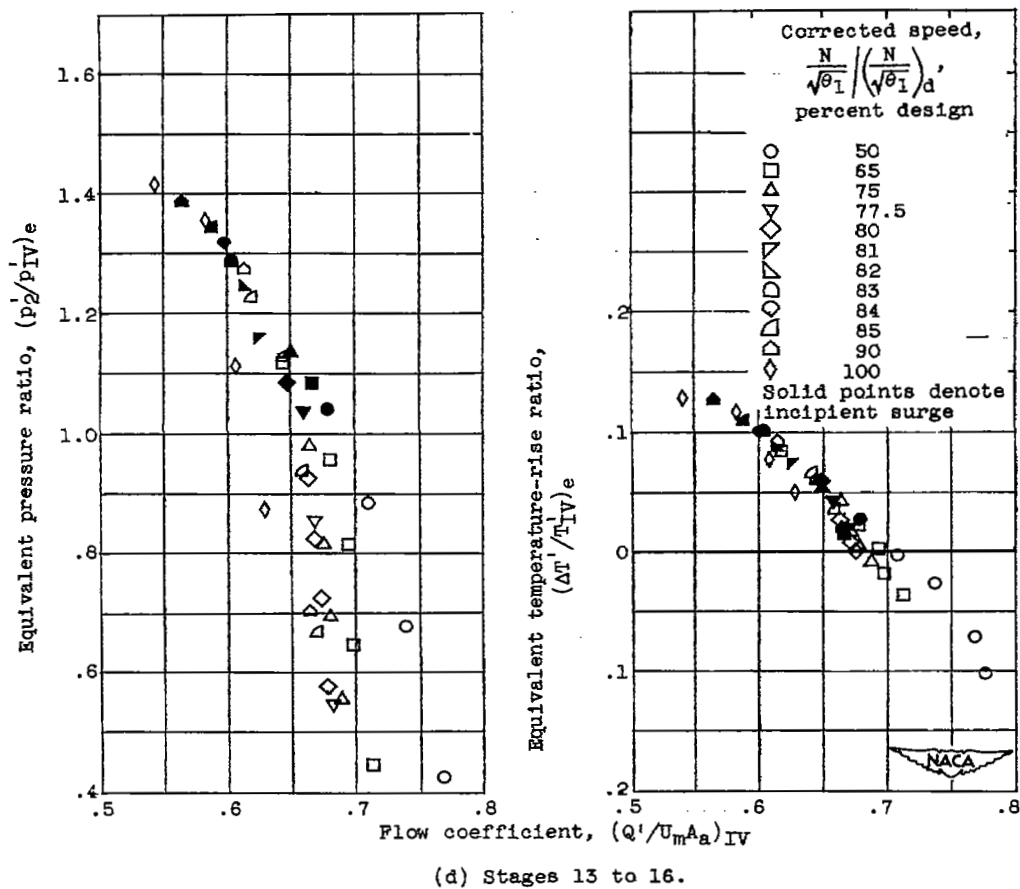


Figure 2. - Concluded. Stage group performance for a 16-stage axial-flow compressor.

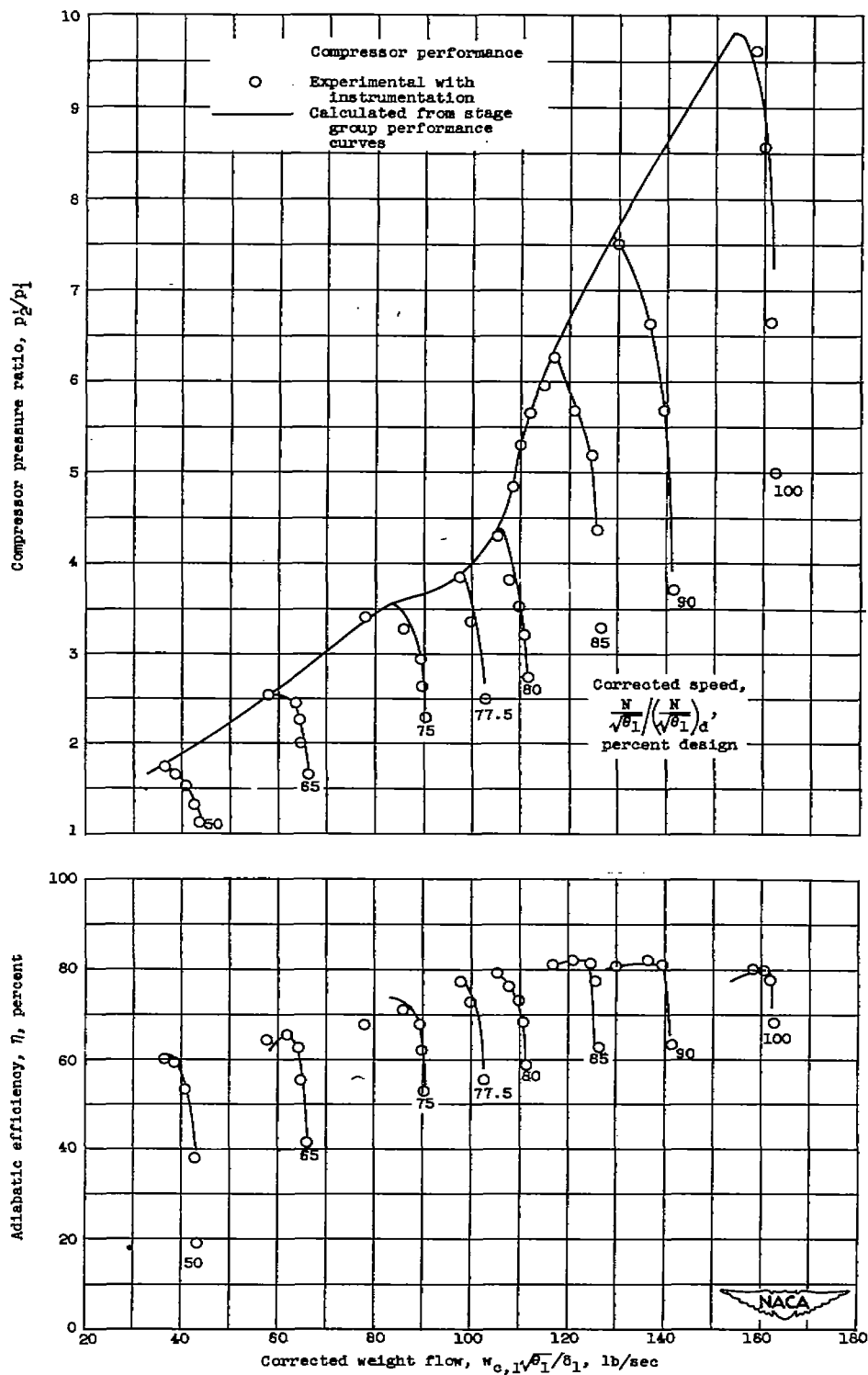
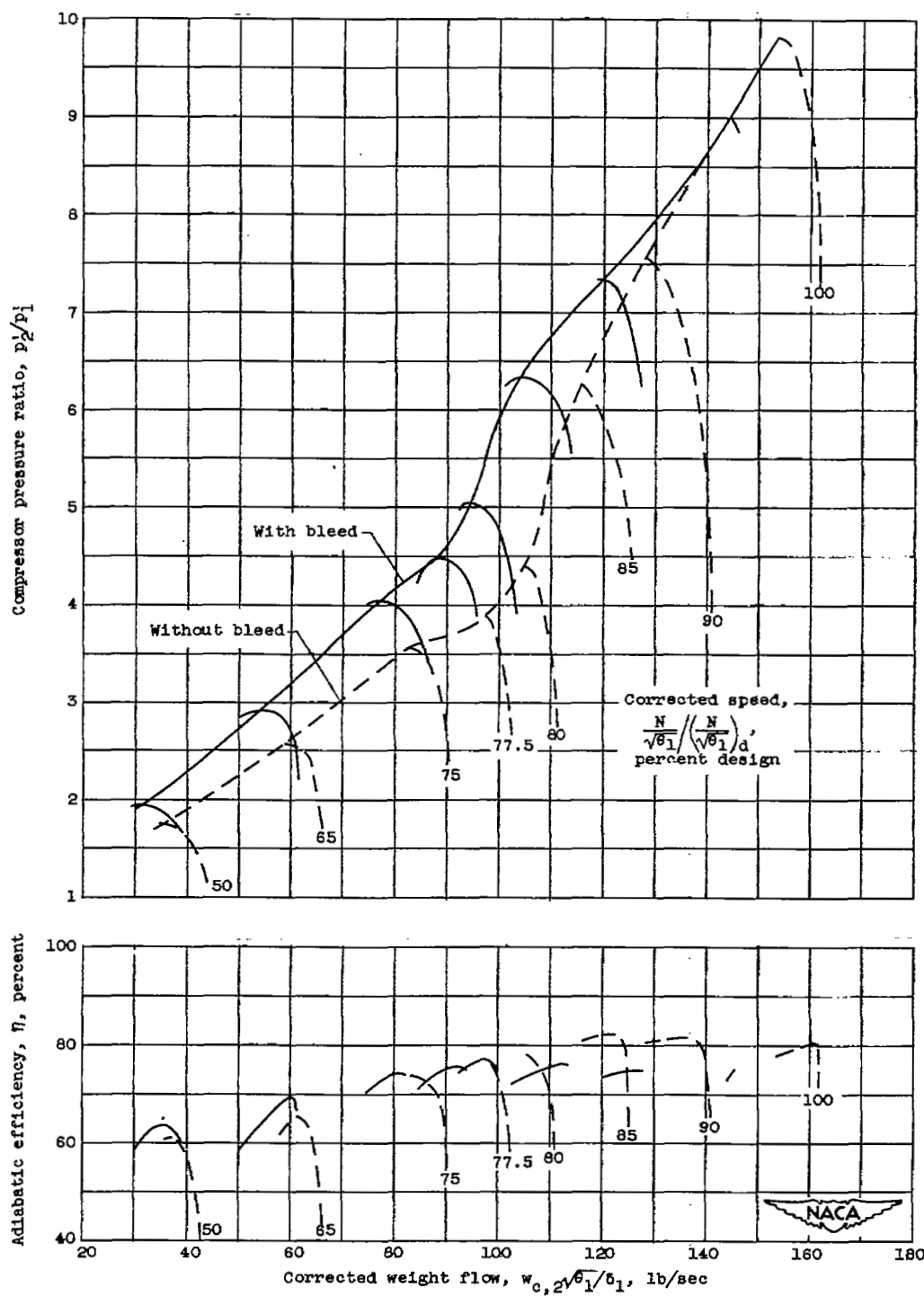


Figure 3. - Comparison of experimental and calculated performance of a 16-stage axial-flow compressor.



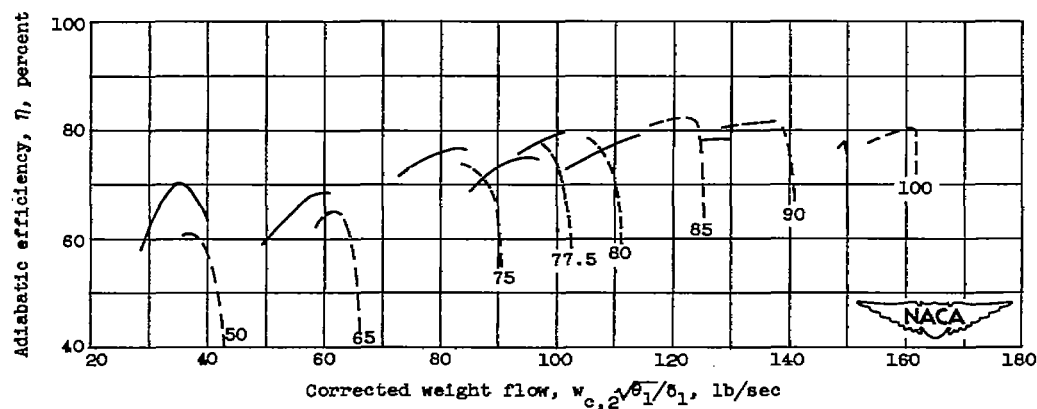
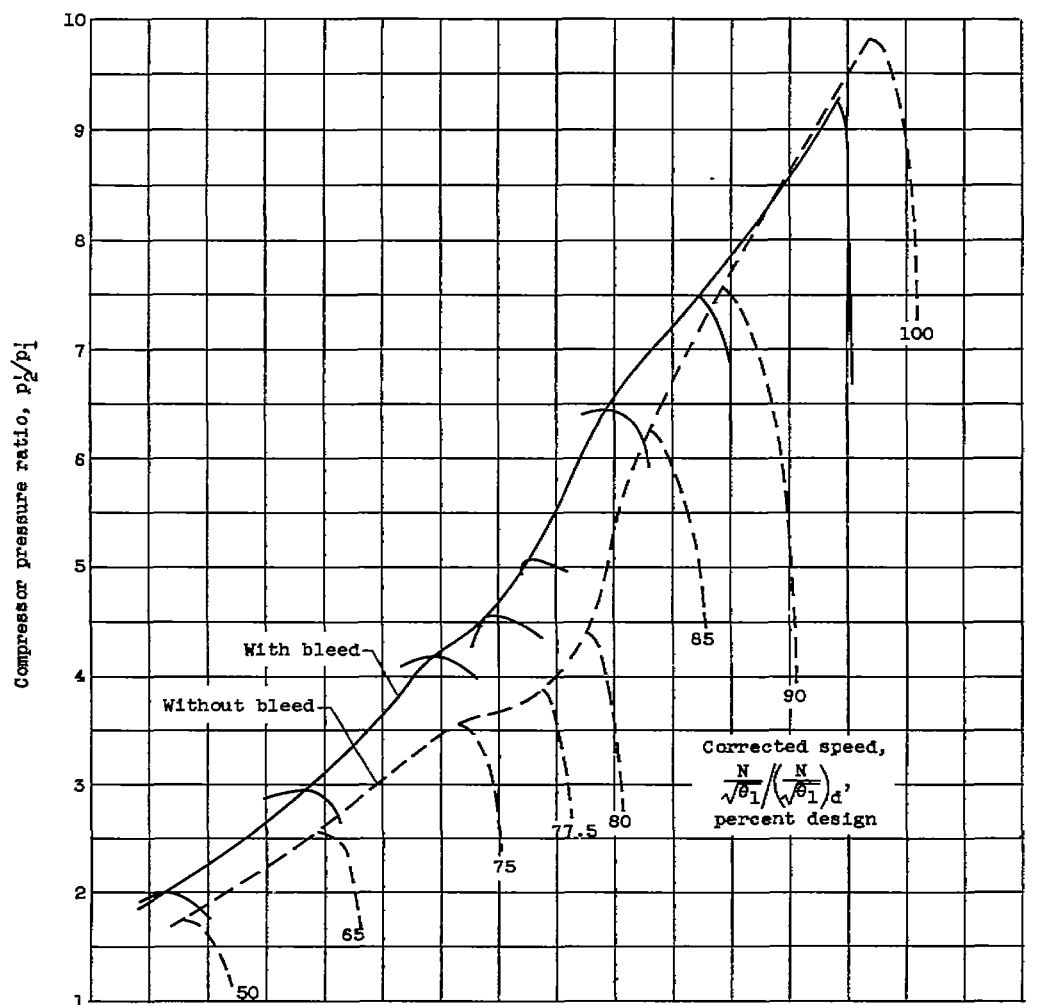


(a) Bleed at exit of 12th compressor stage. Bleed area, 9.5 square inches.

Figure 4. - Comparison of compressor performance with and without interstage bleed.

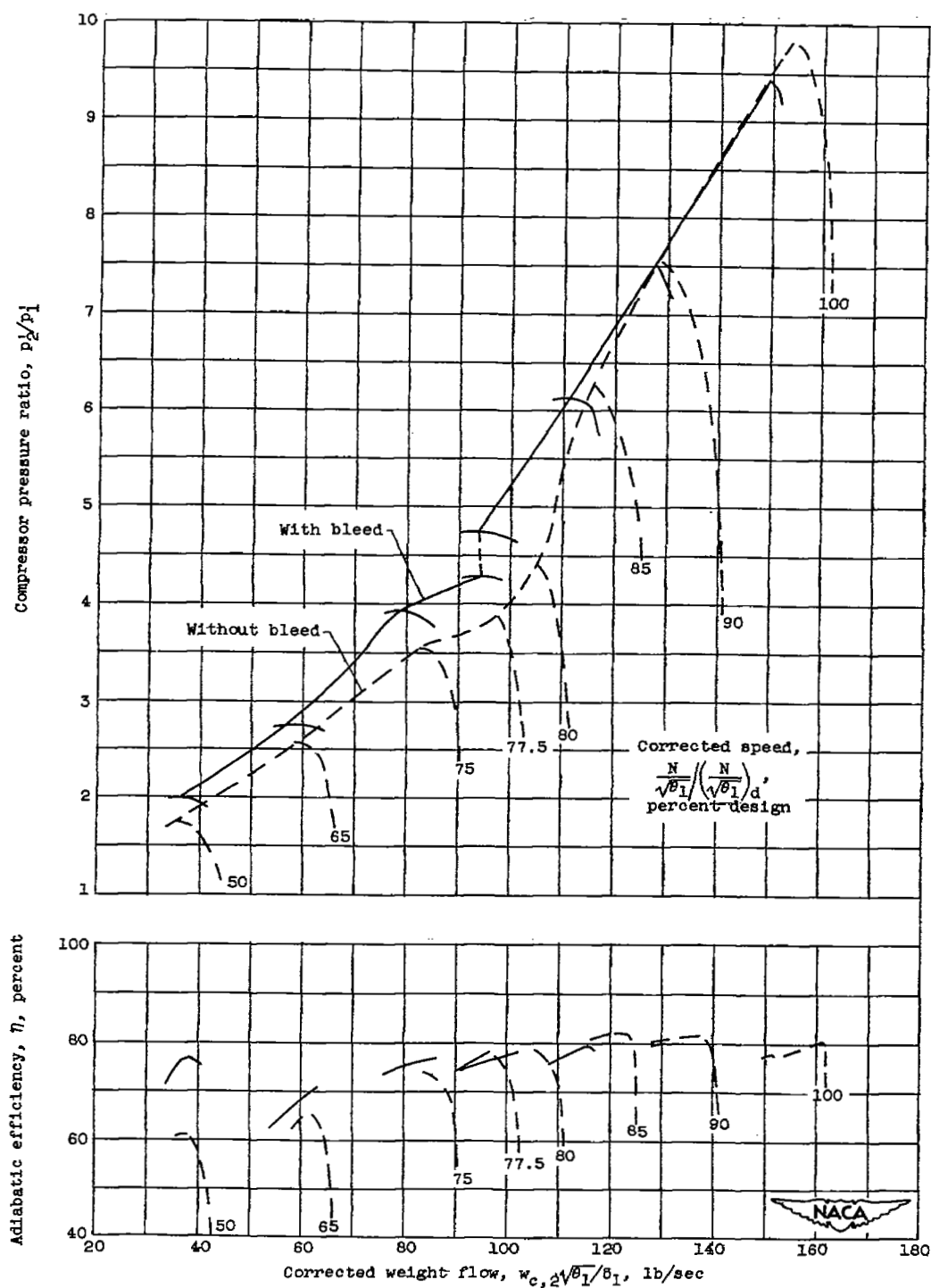
2916

C11-4



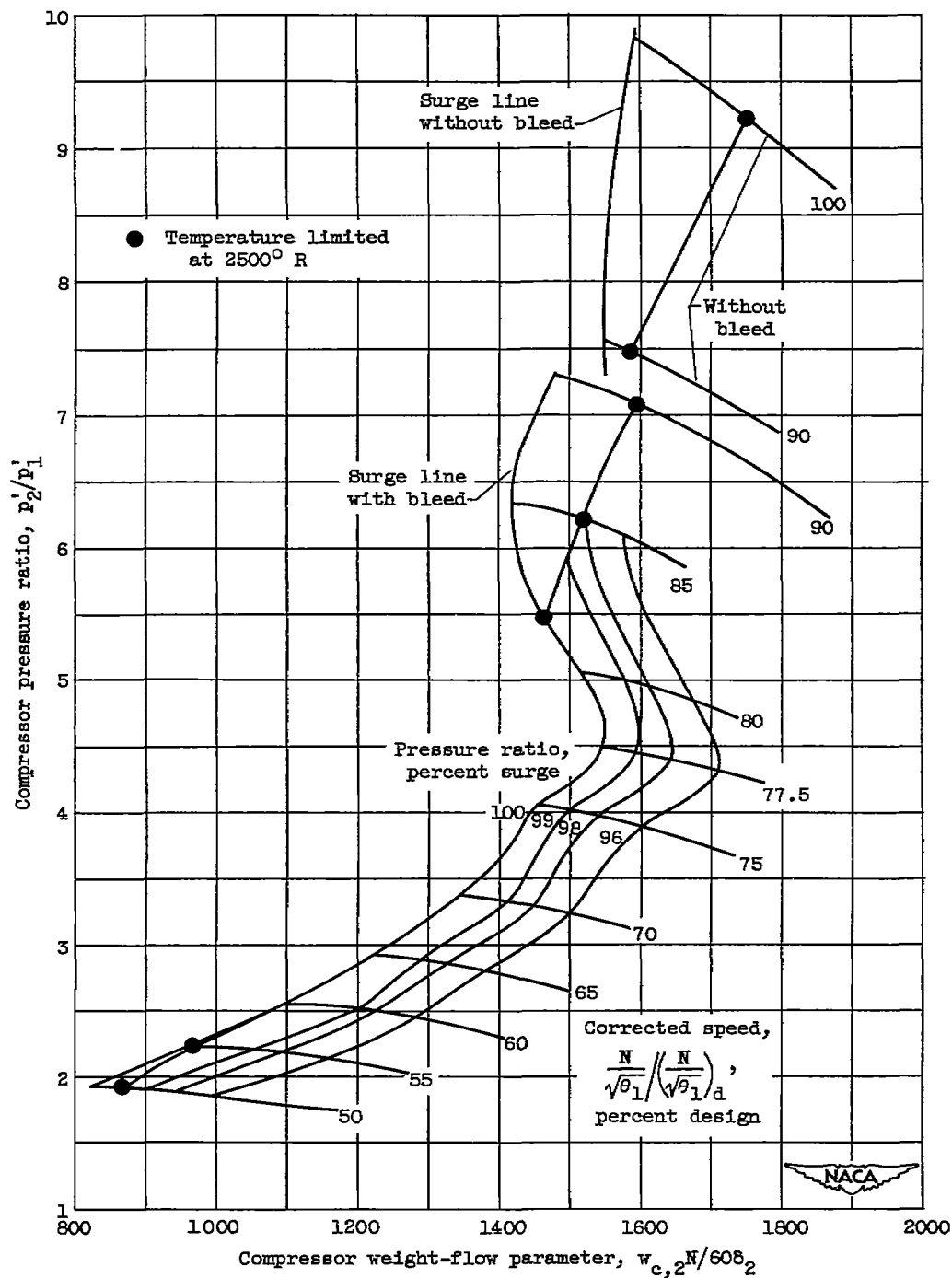
(b) Bleed at exit of 8th compressor stage. Bleed area, 12.0 square inches.

Figure 4. - Continued. Comparison of compressor performance with and without interstage bleed.



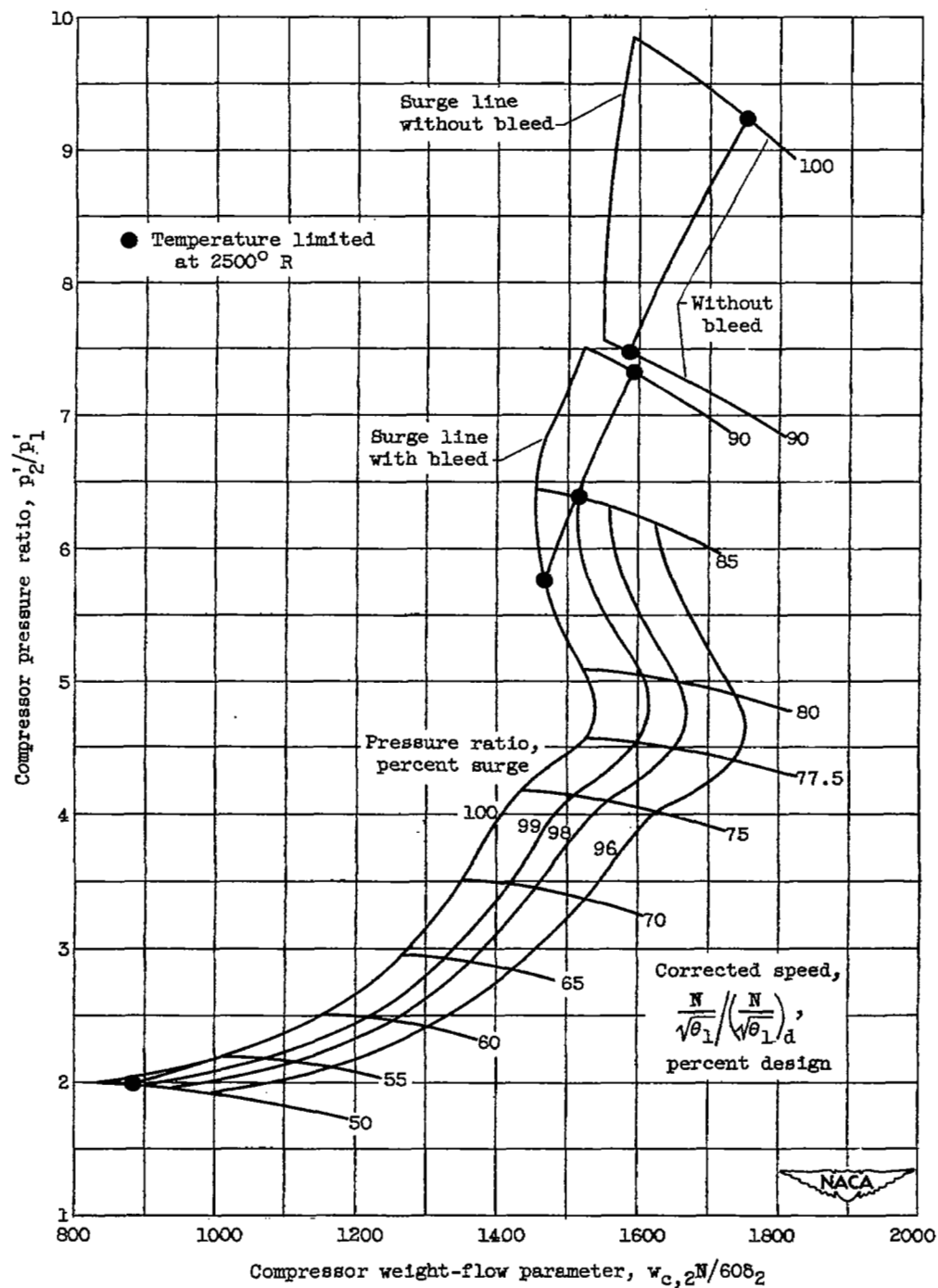
(c) Bleed at exit of 4<sup>th</sup> compressor stage. Bleed area, 17.5 square inches.

Figure 4. - Concluded. Comparison of compressor performance with and without interstage bleed.



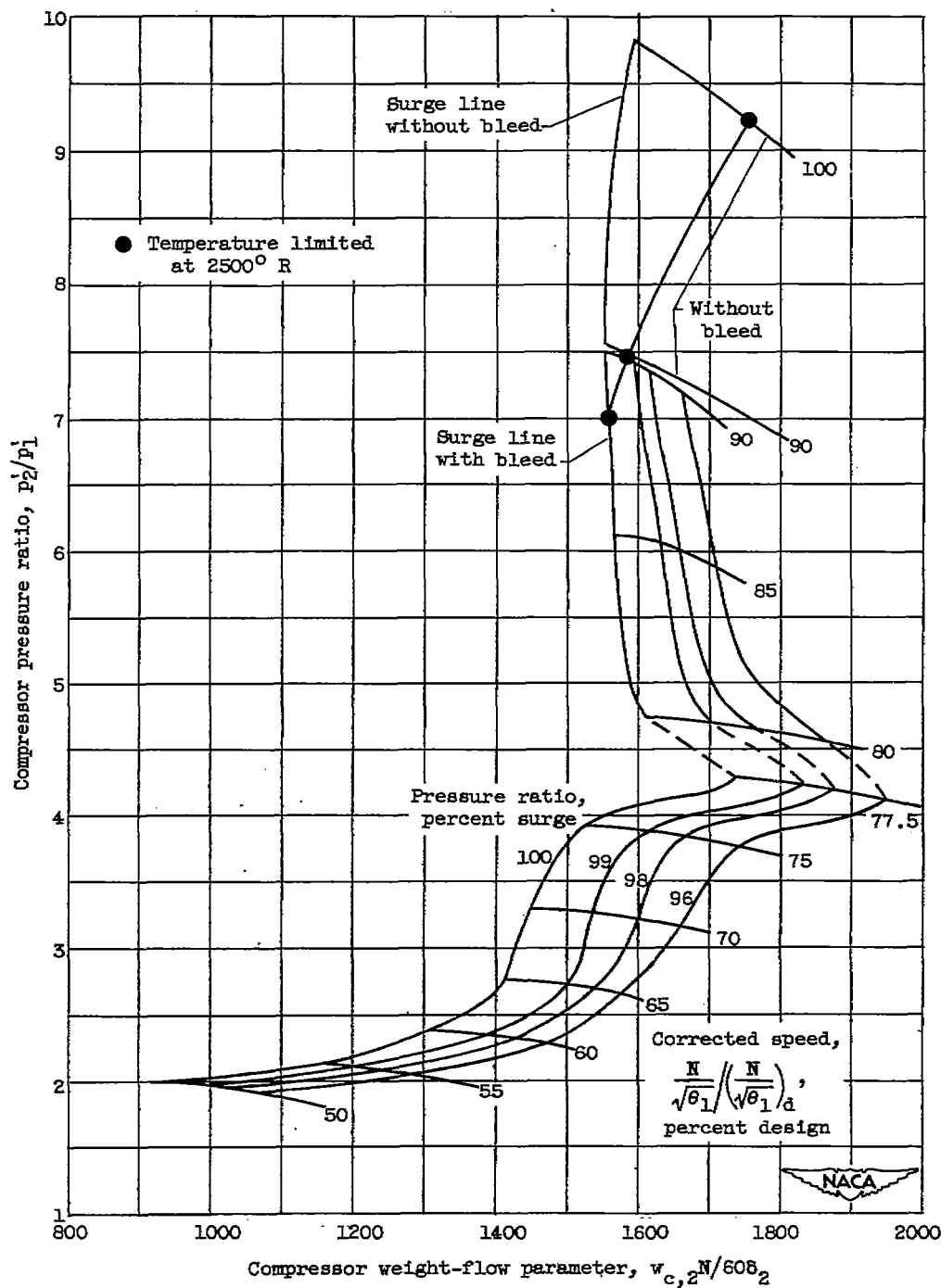
(a) Bleed at outlet of 12<sup>th</sup> compressor stage. Bleed area, 9.5 square inches.

Figure 5. - Engine acceleration paths specified at constant percentage values of surge pressure ratio.



(b) Bleed at outlet of 8th compressor stage. Bleed area, 12.0 square inches.

Figure 5. - Continued. Engine acceleration paths specified at constant percentage values of surge pressure ratio.



(c) Bleed at outlet of 4<sup>th</sup> compressor stage. Bleed area, 17.5 square inches.

Figure 5. - Concluded. Engine acceleration paths specified at constant percentage values of surge pressure ratio.

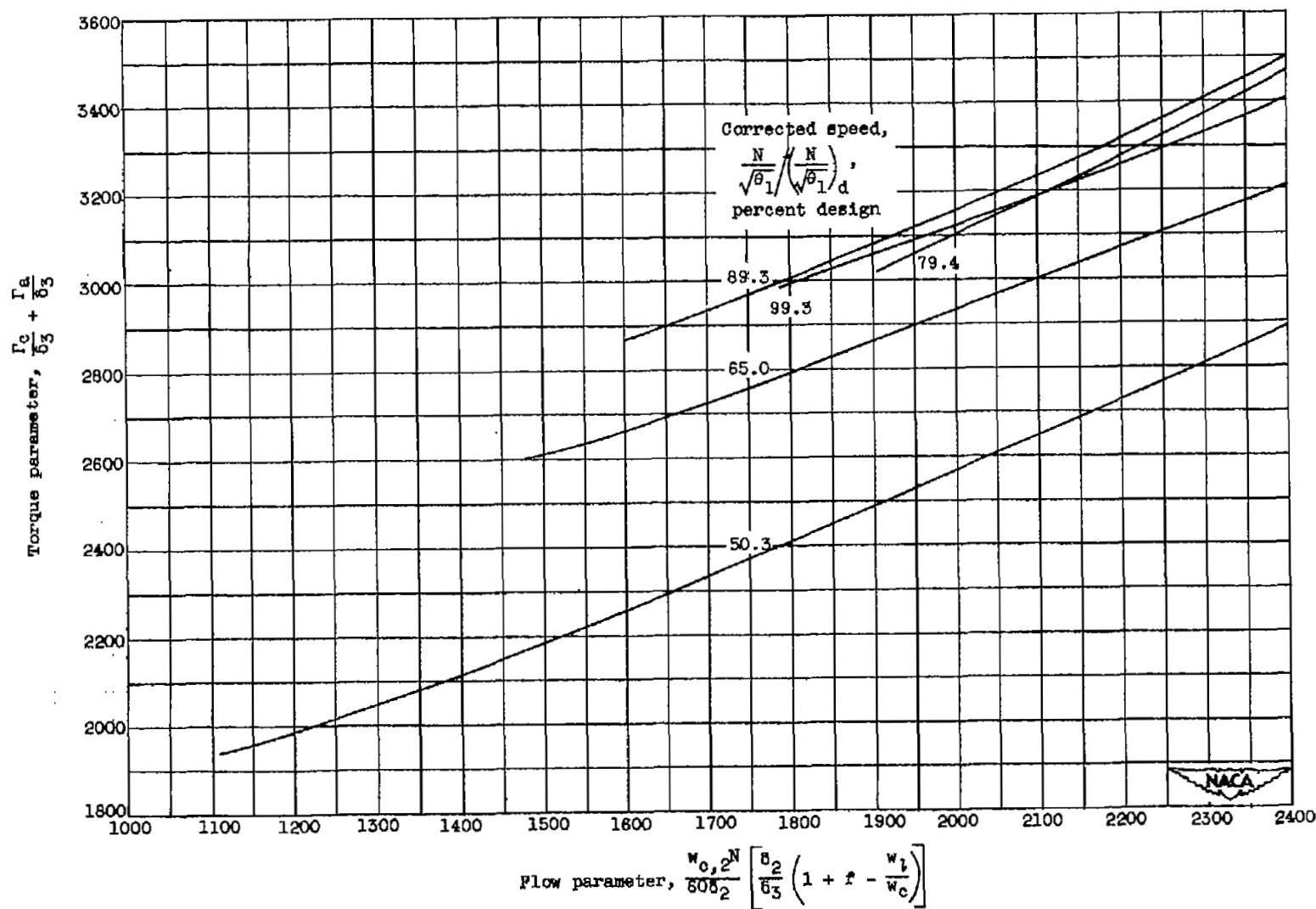


Figure 6. - Compressor torque characteristics.

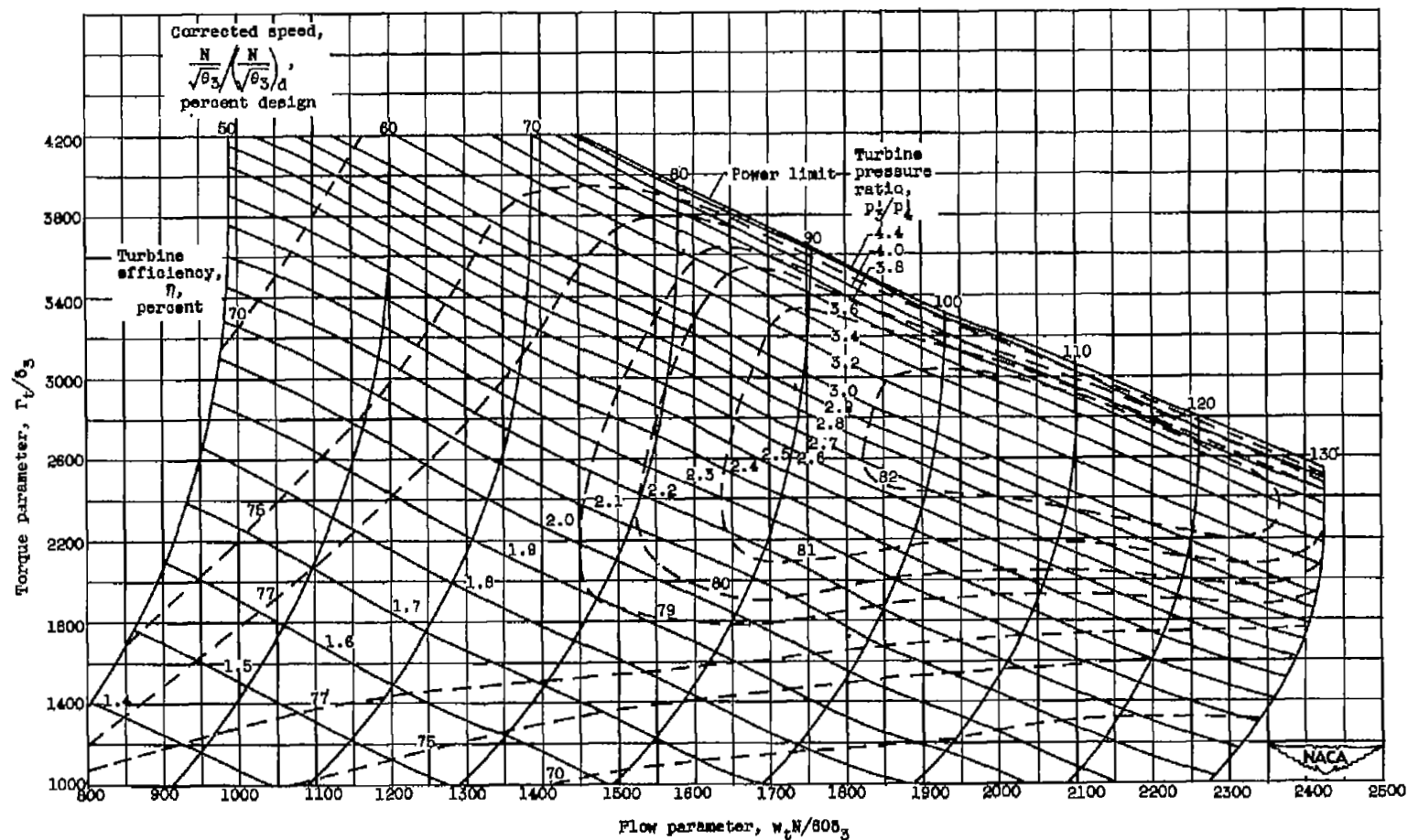


Figure 7. - Turbine performance map.



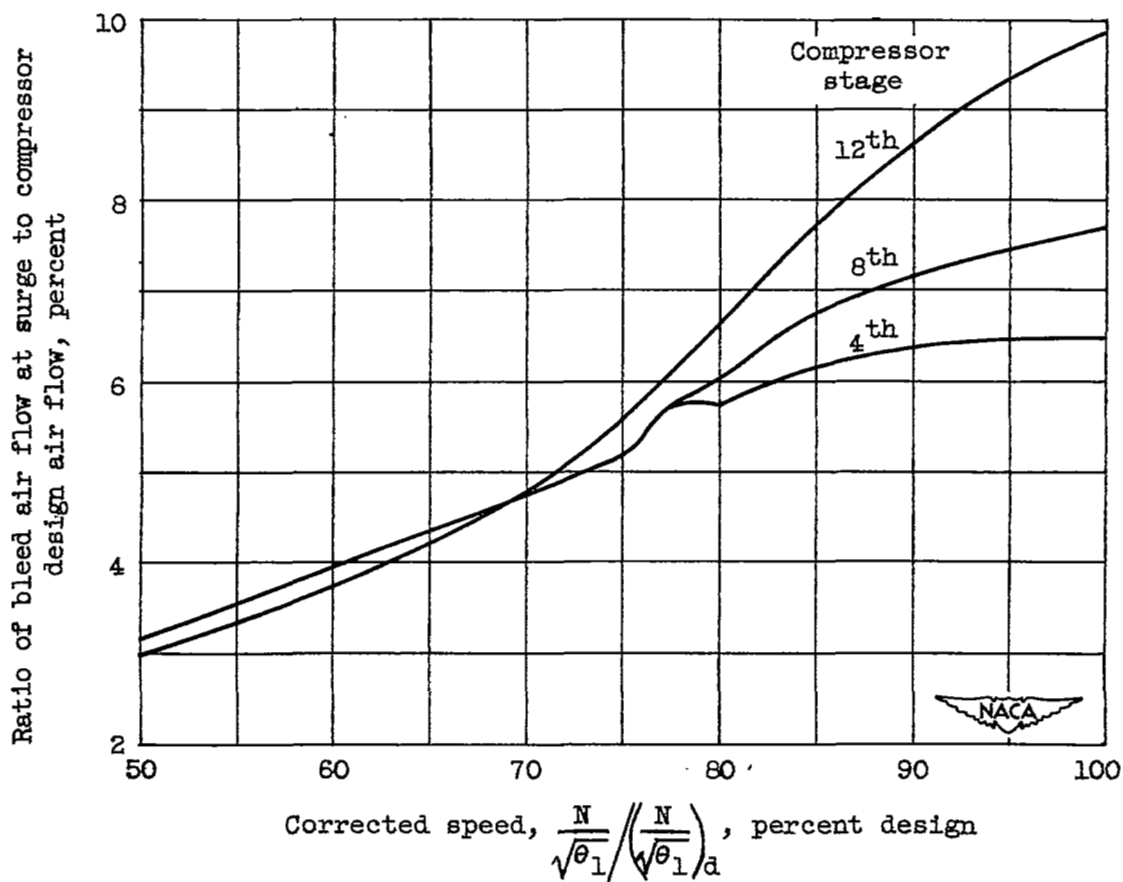
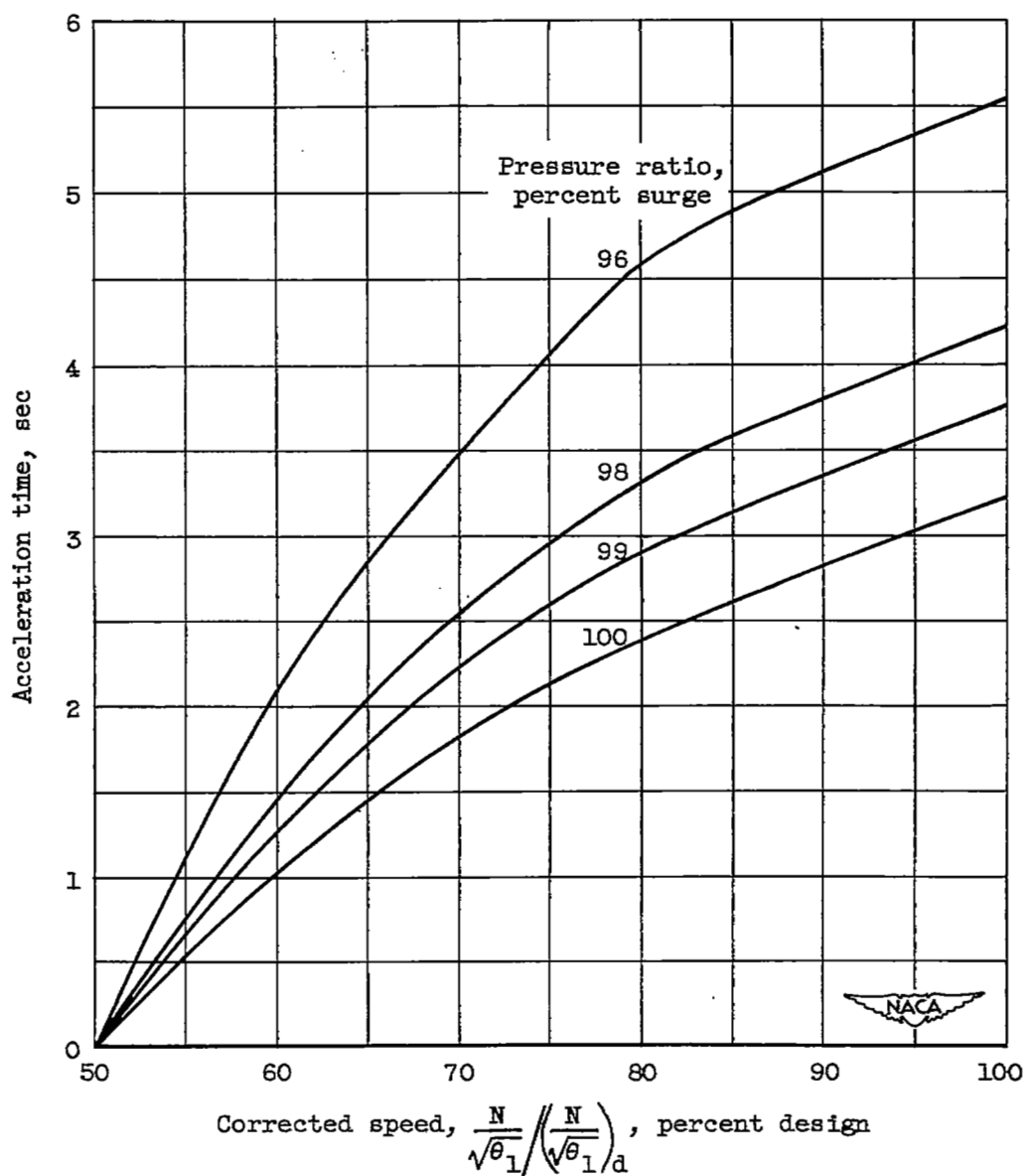
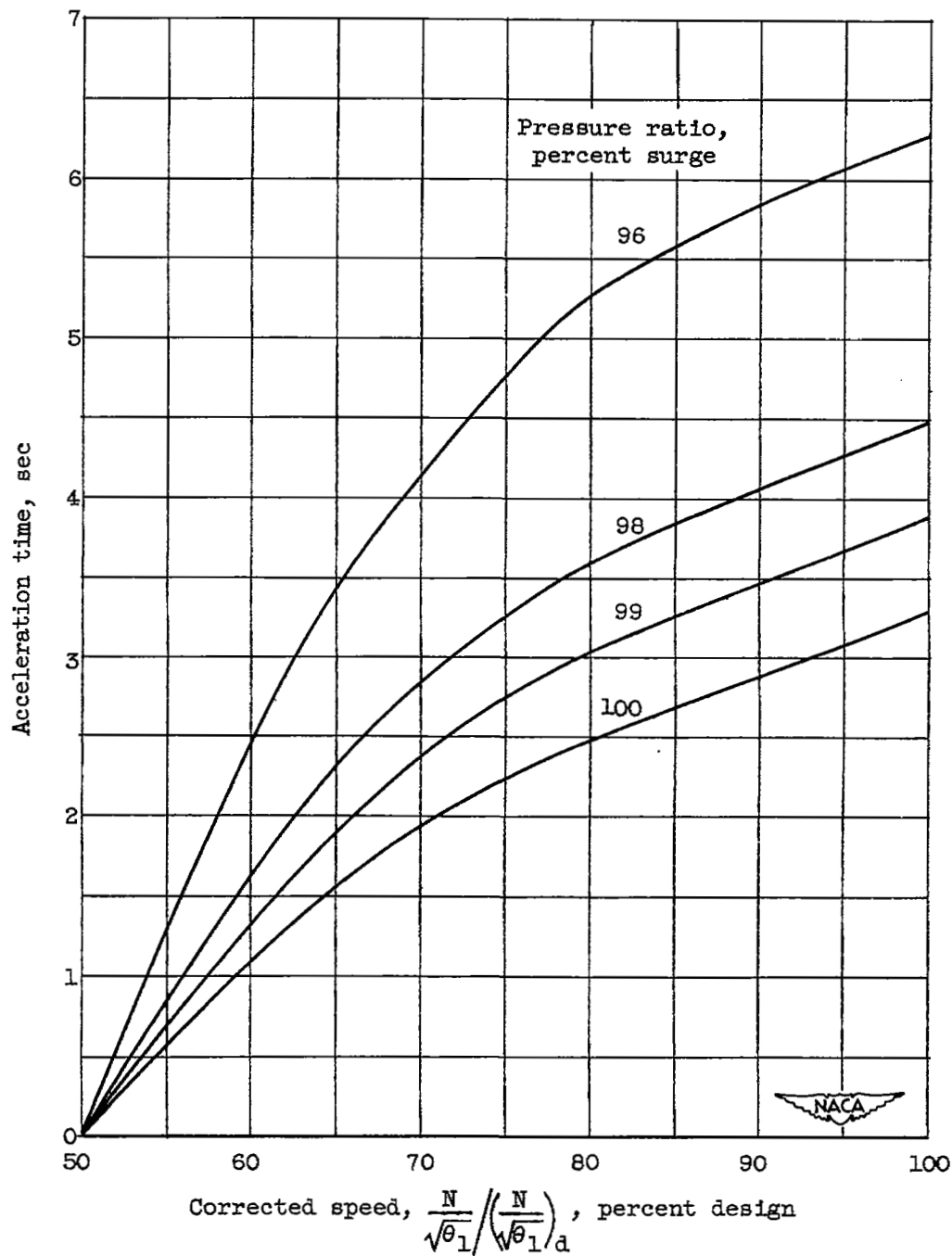


Figure 8. - Comparison of ratio of bleed air flow at surge pressure ratio to compressor design air flow for constant effective bleed areas at the 12th, 8th, and 4th compressor stages.



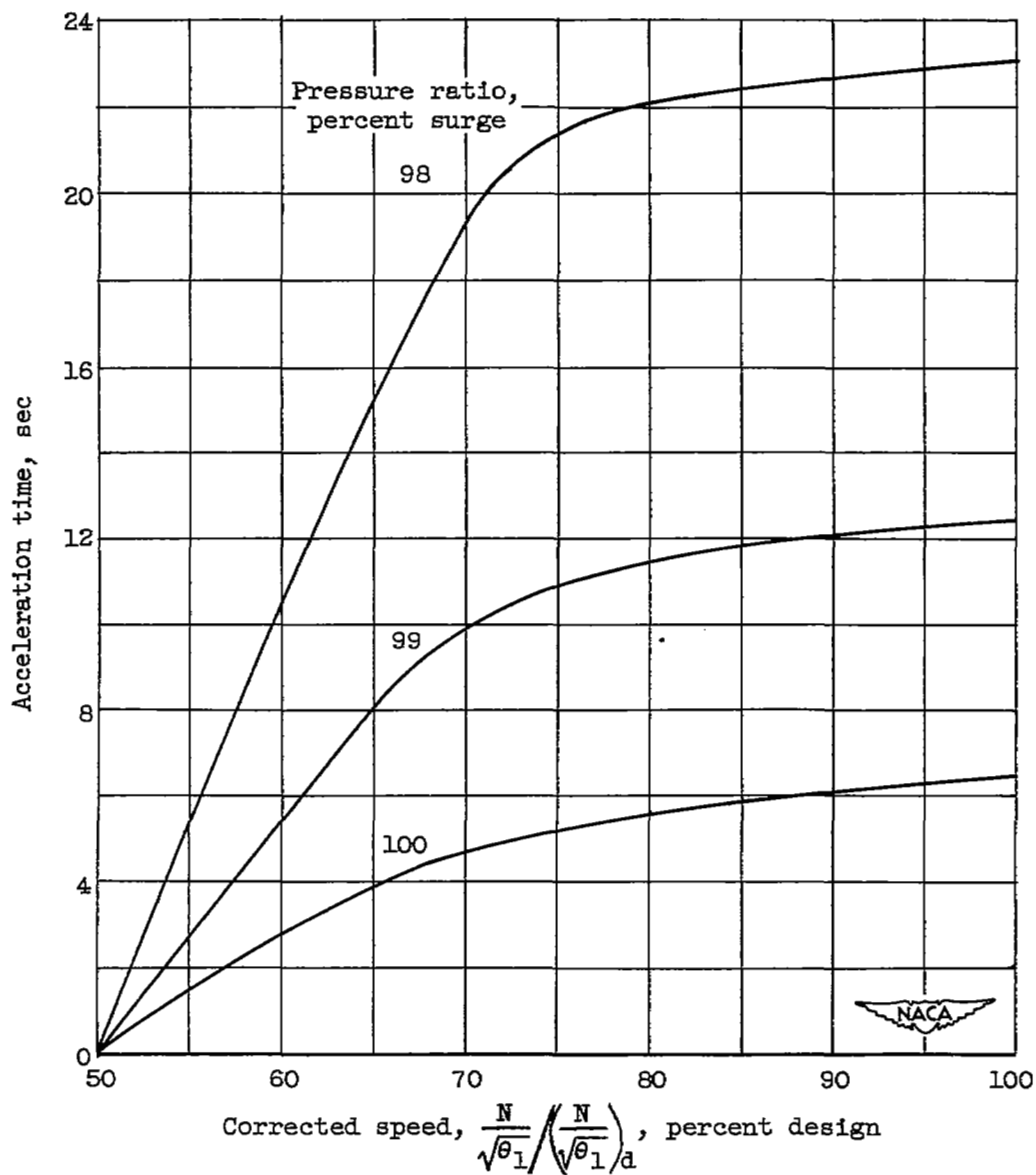
(a) Interstage bleed at 12<sup>th</sup> stage.

Figure 9. - Required acceleration time with interstage bleed at constant percentage values of surge pressure ratio.



(b) Interstage bleed at 8<sup>th</sup> stage.

Figure 9. - Continued. Required acceleration time with interstage bleed at constant percentage values of surge pressure ratio.



(c) Interstage bleed at 4th stage.

Figure 9. - Concluded. Required acceleration time with interstage bleed at constant percentage values of surge pressure ratio.

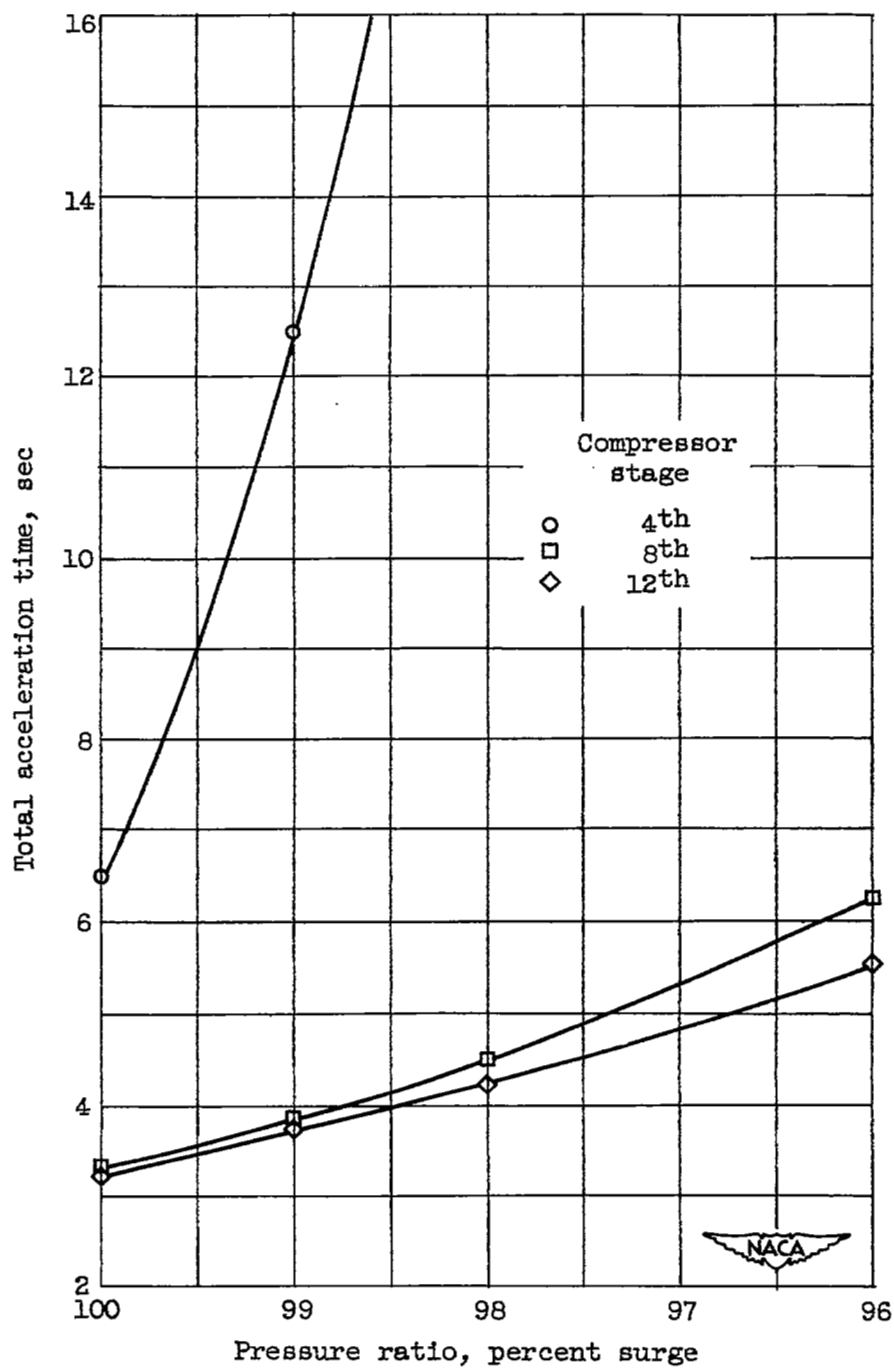


Figure 10. - Total acceleration time for interstage bleed at 4<sup>th</sup>, 8<sup>th</sup>, and 12<sup>th</sup> compressor stages.

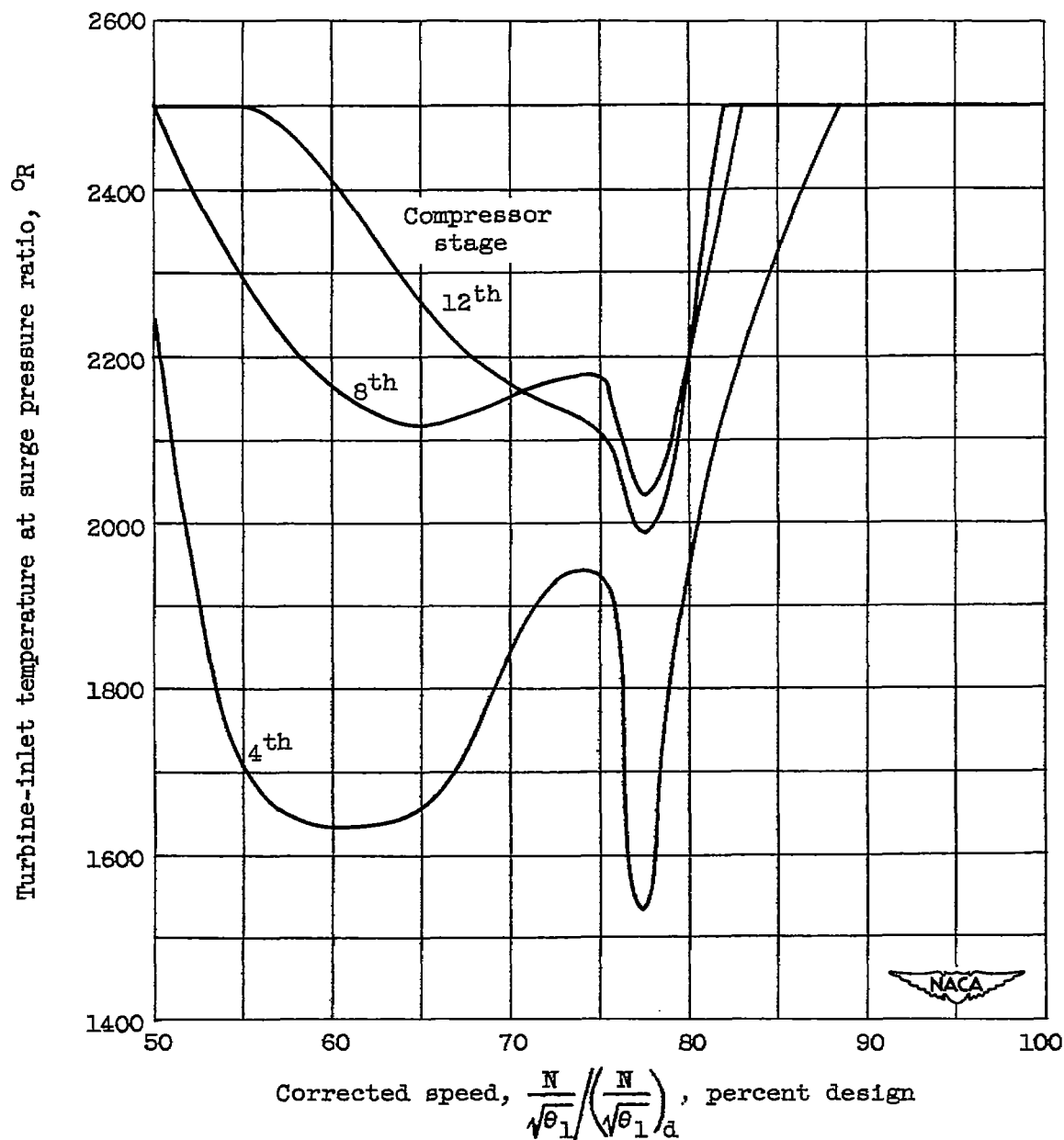


Figure 11. - Variation in turbine-inlet temperature for acceleration at surge pressure ratio with corrected engine speed for bleed at 12th, 8th, and 4th compressor stages.

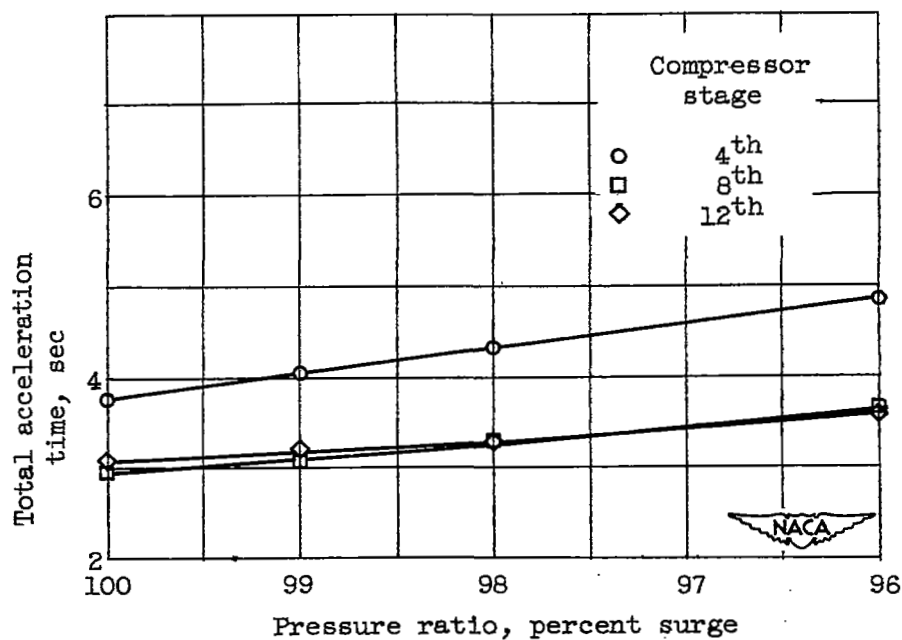


Figure 12. - Total acceleration time for interstage bleed at 4<sup>th</sup>, 8<sup>th</sup>, and 12<sup>th</sup> compressor stages in combination with variable-area bleed at compressor discharge. Turbine-inlet stagnation temperature, 2500° R.

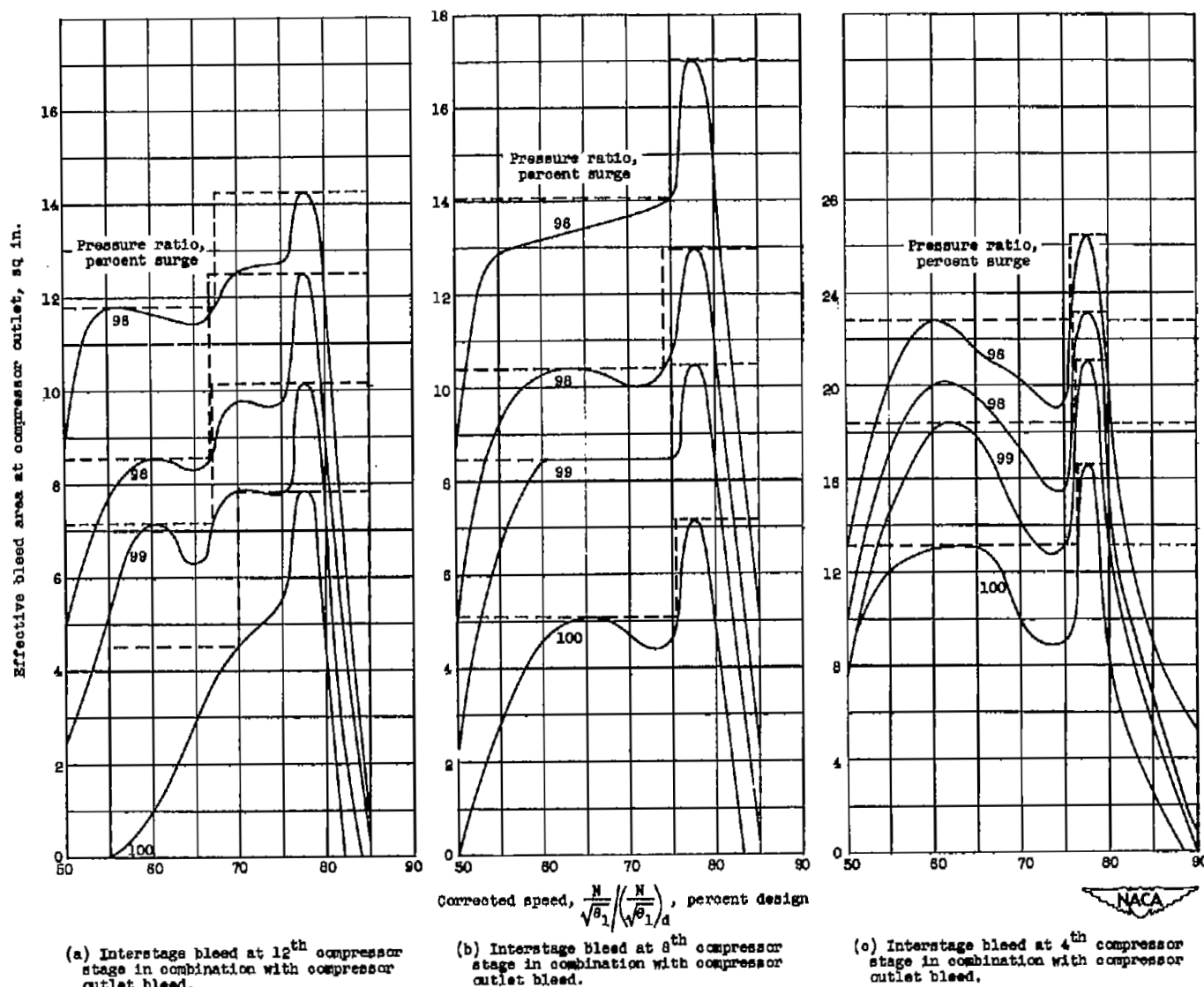


Figure 13. - Area variations at compressor outlet required to maintain a turbine-inlet temperature of 2500° R.



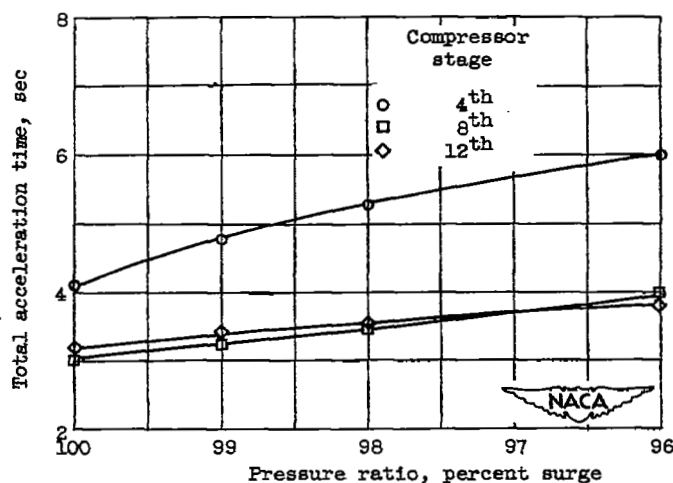


Figure 14. - Total acceleration time for interstage bleed at 4<sup>th</sup>, 8<sup>th</sup>, and 12<sup>th</sup> compressor stages in combination with step-area bleed at compressor discharge. Turbine-inlet stagnation temperature, 2500° R.

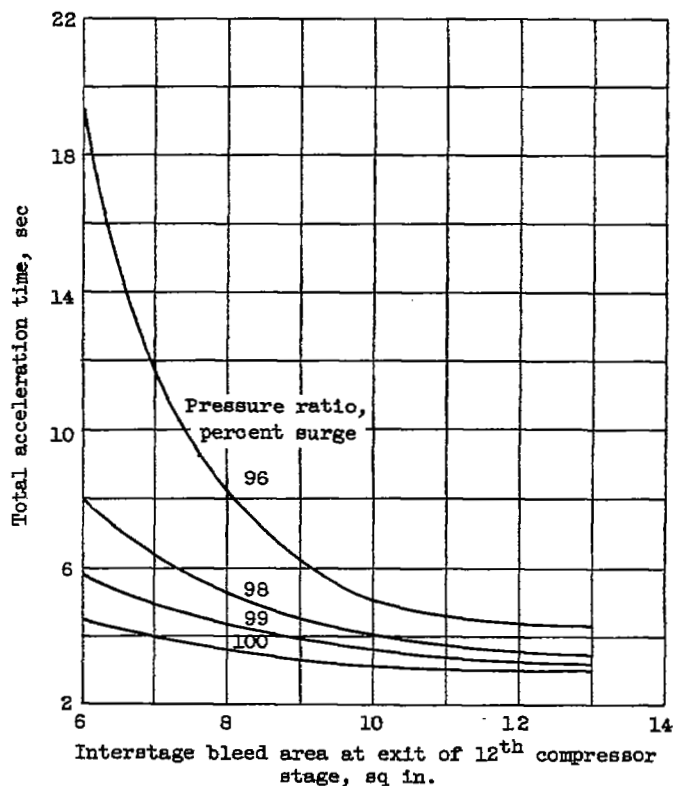
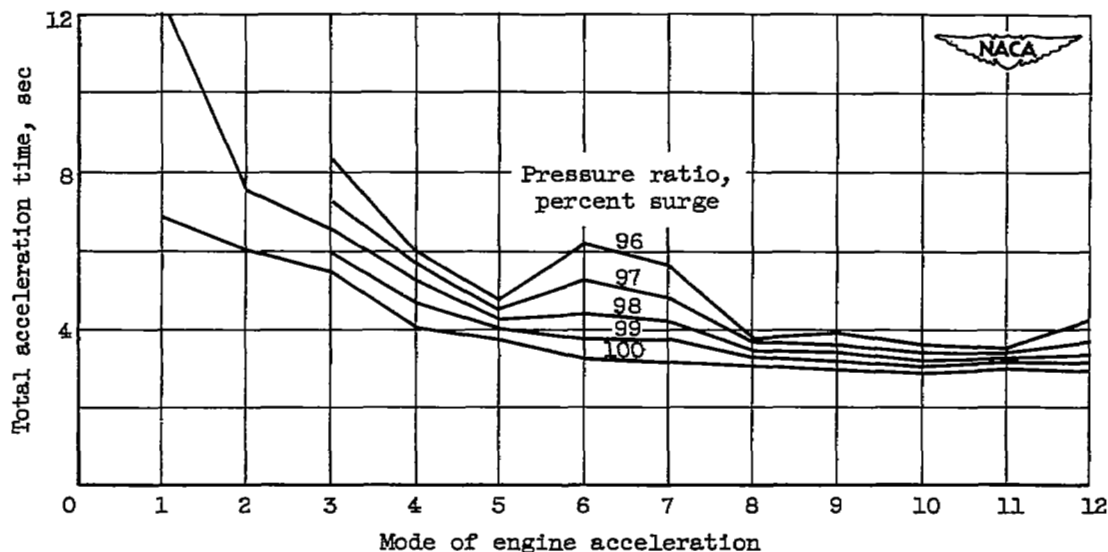


Figure 15. - Variation of total acceleration time with interstage bleed area at exit of 12<sup>th</sup> compressor stage for acceleration paths specified by constant percentage values of surge pressure ratio.



Mode	Interstage bleed		Exit bleed	Turbine-inlet stagnation temperature, $T_3^*$ , OR	Exhaust-nozzle area, $A_5$ , sq in.
	Location, exit of stage	Bleed area, $A_b$ , sq in.	Area variation		
0	(Without bleed, acceleration is not possible)				
1	4 <sup>th</sup>	17.5	-----	Varies	600
2	----	----	Step	2500	600
3	----	----	Continuous	2500	600
4	4 <sup>th</sup>	17.5	Step	2500	600
5	4 <sup>th</sup>	17.5	Continuous	2500	600
6	8 <sup>th</sup>	12.0	-----	Varies	600
7	12 <sup>th</sup>	9.5	-----	Varies	600
8	12 <sup>th</sup>	9.5	Step	2500	600
9	8 <sup>th</sup>	12.0	Step	2500	600
10	8 <sup>th</sup>	12.0	Continuous	2500	600
11	12 <sup>th</sup>	9.5	Continuous	2500	600
12	12 <sup>th</sup>	13.0	-----	Varies	600

Figure 16. - Comparison of acceleration modes. Modes 2 and 3 determined from data of reference 4.

# SECURITY INFORMATION

[REDACTED]



3 1176 01435 7074



[REDACTED]